RESEARCH

Palmitoyl transferases act as novel drug targets for pancreatic cancer

Zhiqing Lin[1,2†], Ziru Lv[2†], Xin Liu[2†] and Keke Huang[1*]

Abstract

Background Pancreatic adenocarcinoma (PAAD) is one of the most leading causes of cancer-related death across the world with the limited efficiency and response rate of immunotherapy. Protein S-palmitoylation, a powerful post-translational lipid modification, is well-known to regulate the stability and cellular distribution of cancer-related proteins, which is mediated by a family of 23 palmitoyl transferases, namely zinc finger Asp-His-His-Cys-type (ZDHHC). However, whether palmitoyl transferases can determine tumor progression and the efficacy of immunotherapy in PAAD remains unknown.

Methods Bioinformatics methods were used to identify differential ZDHHCs expression in PAAD. A systematic pan-cancer analysis was conducted to assess the immunological role of ZDHHC3 using RNA sequencing data from The Cancer Genome Atlas database. In vivo Panc 02 subcutaneous tumor model validated the anti-tumor effect of knockdown of ZDHHC3 or intraperitoneal injection of 2-bromopalmitate (2-BP), a typical broad-spectrum palmitoyl transferases inhibitor. Furthermore, we explored therapeutic strategies with combinations of 2-BP with PD-1/PD-L1-targeted immunotherapy in C57BL/6 mice bearing syngeneic Panc 02 pancreatic tumors.

Results ZDHHC enzymes were associated with distinct prognostic values of pancreatic cancer. We identified that ZDHHC3 expression promotes an immunosuppressive tumor microenvironment in PAAD. 2-BP suppressed pancreatic-tumor cell viability and tumor sphere-forming activities, as well as increased cell apoptosis in vitro, without affecting normal human pancreatic ductal epithelial cells. Furthermore, genetic inactivation of ZDHHC3 or intraperitoneal injection of 2-BP impeded tumor progression in Panc 02 pancreatic tumors with enhanced anti-tumor immunity. 2-BP treatment significantly enhanced the therapeutic efficacy of PD-1/PD-L1 inhibitors in Panc 02 pancreatic tumors.

Conclusion This study revealed some ZDHHC enzyme genes for predicting the prognosis of pancreatic cancer, and demonstrated that ZDHHC3 plays a critical oncogenic role in pancreatic cancer progression, highlighting its potential as an immunotherapeutic target of pancreatic cancer. In addition, combination therapy of 2-BP and PD-1/PD-L1 achieved synergic therapy effects in a mouse model of pancreatic cancer.

Keywords Pancreatic adenocarcinoma, ZDHHC enzymes, ZDHHC3, Immunotherapy

RETRACTED ARTICLE

†Zhiqing Lin, Ziru Lv and Xin Liu contributed equally to the work

*Correspondence:
Keke Huang
kekehuang0714@foxmail.com
[1] Department of Ophthalmology, The Third People's Hospital of Chengdu, The Affiliated Hospital of Southwest Jiaotong University, Chengdu 610031, China
[2] School of Ophthalmology and Optometry, Eye Hospital, Wenzhou Medical University, Wenzhou 325027, China

Introduction

Pancreatic adenocarcinoma (PAAD) is among the most aggressive and lethal human malignancies that occur with poor prognosis, which causes over 331,000 cancer-related death per year worldwide [1]. Long-term survival in resectable disease will be improved by surgical resection and adjuvant chemotherapy, but the majority of PAAD patients are diagnosed at an advanced and fatal stage with consequent loss of therapeutic opportunity

Lin *et al. Journal of Translational Medicine*   (2023) 21:249

Page 2 of 24

[2]. Advanced PAAD is non-operable and notorious for its resistance to chemoradiotherapy, reaching a 5-year overall survival (OS) rate below 10% in the USA [1, 3]. Thus, there remains an urgent requirement to discover novel prognostic biomarkers and develop effective therapeutic strategies for PAAD.

Emerging evidence has indicated that the tumor immune microenvironment differentially participates in the pathogenesis of PAAD and influences the clinical outcomes of patients [4]. PAAD patients are predominantly represented by a "cold" tumor microenvironment (TME) with limited infiltrating immune cells, which is characterized by hypoxia and extensive stromal and matrix deposition (desmoplasia) [4, 5]. Increased percentage of immunosuppressive cells and lack of infiltration of natural killer (NK) cells and cytotoxic T lymphocytes contribute to the highly immunosuppressive TME [6, 7]. Currently, immunotherapeutic strategies (e.g., immune checkpoint blockade therapy, combinatorial approach with other immunotherapeutic agents or targeted molecular agents, etc.) have been applied in many solid tumor types due to its excellent efficacy and clinical safety [8]. Especially immune checkpoint inhibitors targeting programmed cell death-1 (PD-1) and its ligand-1 (PD-L1) have dramatically revolutionized the cancer treatment landscape and represented the cornerstone of immunotherapy [9, 10]. However, PD-1/PD-L1 blockade has so far demonstrated a modestly therapeutic effect in PAAD patients [11]. Thus, there is an urgent unmet clinical need to further explore potential molecular targets for pancreatic cancer initiation and progression and to identify effective therapeutic strategies to enhance PAAD patients' responsiveness to immunotherapy.

Protein lipidation events are a prototypical form of post-translational modification, in which S-palmitoylation exerts multiple effects to dynamically orchestrate the target protein interaction. It involves the reversible attachment of C16 palmitic acid to cysteine residues through thioester bonds [12]. About 10% of the proteome is prone to S-palmitoylation through palmitoylate screens and prediction [13]. Dynamic S-palmitoylation events provide a vital mechanism for modulating protein stability, localization, conformation, intracellular trafficking, and function by altering membrane affinity [14–16]. Of note, a large number of cancer-related mammalian proteins with S-palmitoylated internal cysteine residues have been identified [17]. The majority of S-palmitoylated proteins are catalyzed by a group of zinc finger Asp-His-His-Cys-type (ZDHHC) enzymes [18]. Thus, the key to identifying palmitoyl transferase's role in pancreatic cancer is the systemic evaluation of ZDHHC family members. Several ZDHHC

enzymes are highly expressed in the brain, thus, S-palmitoylation has been widely reported in neuronal systems. More recent works focus on the role of S-palmitoylation in the immune pathways and cancer [12, 19]. Hence, targeting ZDHHC enzymes may provide a novel insight into the underlying molecular mechanisms of immunotherapy resistance and offer strategies for pancreatic cancer immunotherapy.

There is an established link between S-palmitoylation and cancer [20–22]. Recently, the application of targeting S-palmitoylation in cancer therapy has been widely studied, for instance, genetic inhibition of ZDHHC family members (e.g., ZDHHC3, ZDHHC5, ZDHHC17, ZDHHC9, and ZDHHC12) have shown promising and enhanced anticancer effects in colon cancer, breast cancer, non-small cell lung cancer, glioma, leukemia, and ovarian cancer [23–30], while genetic activation of ZDHHC13 exhibits protective effects in skin cancer [31]. However, the potential functions of ZDHHC family members in pancreatic cancer development remain largely undefined.

To address this problem, we first aimed at investigating the key ZDHHCs involved in PAAD through the analysis of prognostic value associated with the expression patterns of the ZDHHC family of genes. Then we screened and validated the expression of ZDHHC3 was significantly upregulated and associated with poor prognosis of patients with PAAD. Moreover, we investigated the immunological significance of ZDHHC3 through a comprehensive analysis of pan-cancer transcriptomic data and observed that ZDHHC3 was inversely correlated with anti-tumor immunity in PAAD. Knockdown of tumor cell ZDHHC3 expression or intraperitoneal injection of 2-bromopalmitate (2-BP), a typical broad-spectrum palmitoyl transferases inhibitor, slowed the Panc 02 tumor growth with enhanced anti-tumor immunity. Notably, 2-BP treatment significantly enhanced the therapeutic efficacy of PD-1/PD-L1 inhibitors in Panc 02 pancreatic tumors (Scheme 1). Together, the present findings suggest that ZDHHC3 plays an essential oncogenic role in pancreatic cancer and propose the combination therapies of 2-BP and PD-1/PD-L1 blockade agents to facilitate checkpoint immunotherapy in pancreatic cancer.

Materials and methods
Scheme 1 shows the overall workflow of this study

Datasets
Gene Expression Profiling Interactive Analysis (GEPIA: http://gepia2.cancer-pku.cn/) database is an interactive web application tool that furnishes a platform for the analysis of differential gene expression profile and
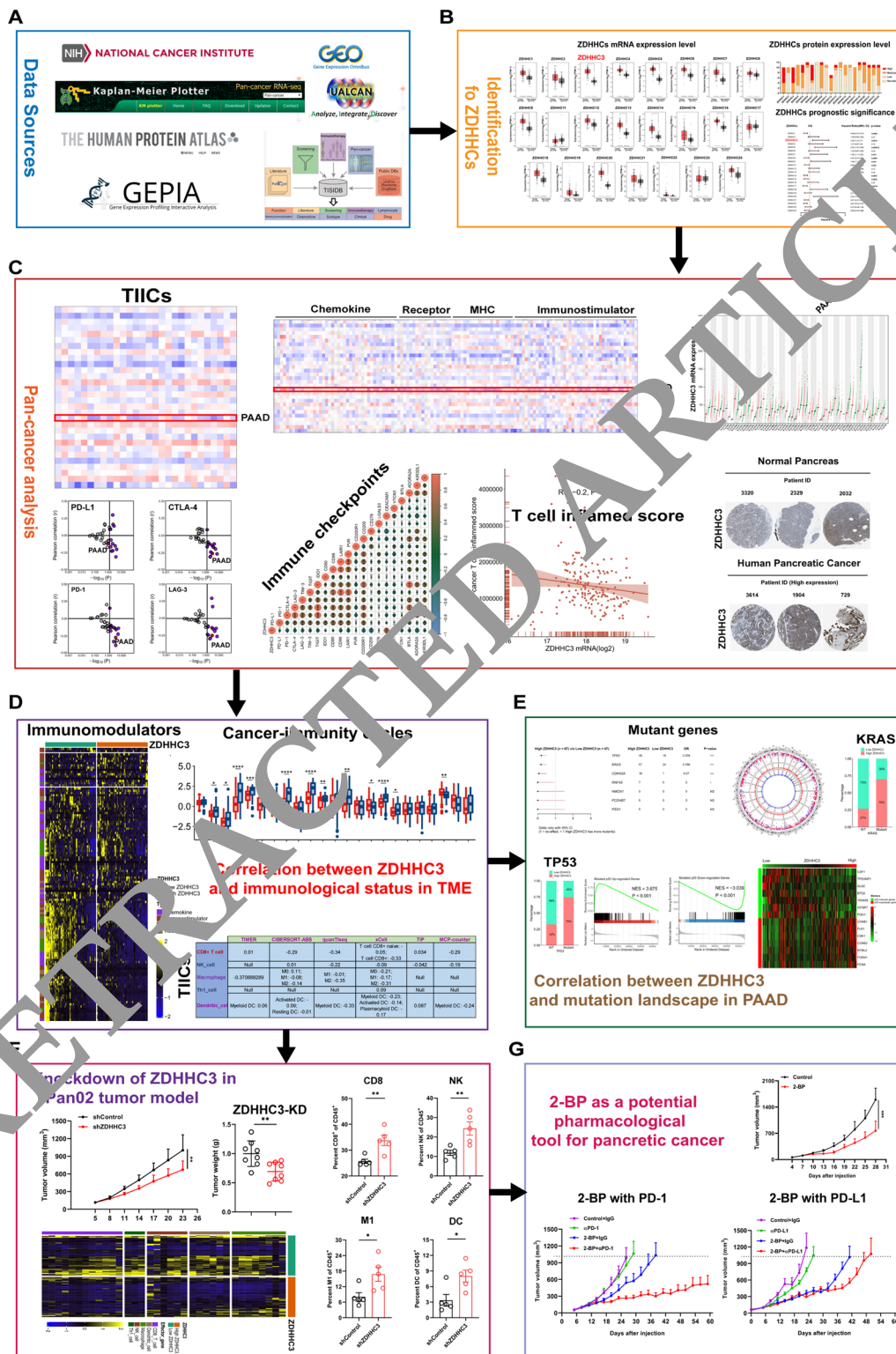
Scheme 1 Schematic overview of the experimental design. **A** Various sources of data used in the principal part of this study. **B** Identification of pancreatic cancer-related ZDHHC. **C** Pan-cancer analysis examining correlations between ZDHHC3 mRNA levels and immunological elements. The relative infiltrations of TIICs in the TME were analyzed using the ssGSEA algorithm. **D** Correlation between ZDHHC3 mRNA levels and the immunological profiles of the TME in PAAD. **E** The relationships between ZDHHC3 expression and mutation landscape in TCGA-PAAD cohort. **F** Genetic targeting ZDHHC3 in Panc 02 tumor model. **G** Pharmacological targeting ZDHHCs for pancreatic cancer treatment. TIICs: tumor-infiltrating immune cells; KD: knockdown; TME: tumor microenvironment

Lin *et al. Journal of Translational Medicine* (2023) 21:249

Page 4 of 24

pathological status using TCGA and the GTEx (Genotype-Tissue Expression) dataset [32]. In our study, visual analysis of ZDHHCs gene expression, prognostic value, and the pathological stage was performed using the "TCGA-PAAD" dataset in GEPIA. In addition, the ZDHHC3 pan-cancer expression profile in tumor and non-tumor tissues was analyzed using TCGA data as well as the GTEx database.

The Human Protein Atlas (HPA: https://www.proteinatlas.org/) provides a user-friendly web resource for investigating the protein level of ZDHHCs and differentially expressed ZDHHC3 in PAAD tumor and non-tumor samples. To investigate differences in the protein expression levels of ZDHHCs and the differentially expressed ZDHHC3 in PAAD tumor and non-tumor tissues, we explored the publicly available Human Protein Atlas.

The Gene Expression Omnibus (GEO: https://www.ncbi.nlm.nih.gov/geo/) project is a public platform for gene expression datasets [33]. We downloaded two PAAD GEO cohorts, namely GSE15471, and GSE16515 to evaluate the differential expression profile of ZDHHC3 between the pancreatic cancer tissue samples and normal pancreatic tissue samples.

UALCAN (http://ualcan.path.uab.edu/) is an open-access web portal, with the aim to analyze large-scale transcriptome clinical patient data from the Clinical Proteomic Tumor Analysis Consortium (CPTAC) cohort (https://proteomics.cancer.gov/programs/cptac) [34]. The protein abundance of ZDHHC3 was explored in this study from CPTAC-PAAD proteomic data.

The web version of Kaplan–Meier Plotter (K-M plotter: http://kmplot.com/) [35] provides direct access to perform survival time analysis and was utilized to analyze the prognostic values of ZDHHCs in PAAD. TCGA-PAAD patients were classified into high and low ZDHHC3 two groups according to the median values of ZDHHC3 expression and overall survival (OS) and progression-free survival (PFS) were calculated. Additionally, hazard ratios (HRs) were calculated with 95% confidence intervals (CIs). Log-rank p-values were autogenerated on the platform.

In particular, to reveal the potential genes which were markedly positively associated with ZDHHC3 gene expression, signaling pathway enrichment analysis was performed using the Kyoto Encyclopedia of Genes and Genomes (KEGG). The KEGG pathways were enriched and visualized through the R package 'cluster Profiler' at $P < 0.05$ (R version 4.2.1). Specifically, the scores of ssGSEA were executed using the Gene Set Variation Analysis (GSVA) R package with the parameter method 'ssgsea'. Meanwhile, the correlations between ZDHHC3

and P53 pathway scores were analyzed by the Spearman rank correlation test.

Evaluation of the immunological characteristics of the TME in PAAD

The TISIDB database (http://cis.hku.hk/TISIDB/) was utilized to explore the correlations between ZDHHC3 expression and 124 immunomodulators and 28 cancer-associated immune cells. We computed a pan-cancer immune cell infiltration score, which plays a critical role in determining anti-cancer immunity and predicting the response to immune checkpoint blockade. To estimate the correlation with ZDHHC3 mRNA expression, ZDHHC3 mRNA expression levels above the 60th quartile were defined as high, and below the 40th quartile were defined as low. Based on the pan-cancer gene expression data from TCGA, we calculated the Pearson correlation between the mRNA levels of four immune checkpoint genes (PD-L1, CTLA-4, PD-1, and LAG-3) and ZDHHC3. All cases in TCGA-PAAD were divided into two groups: high ZDHHC3 expression and low ZDHHC3 expression groups, and FPKM data were collected on 124 immuno-modulators (including immunostimulants, major histocompatibility complex (MHC) molecules, receptors, and immune-relevant chemokines) from the TCGA-PAAD cohort, finally, the heat map representation of fold-change of gene expression profiles was formed using the "ComplexHeatmap" R software package. Evaluation of cancer immunity cycle activity was performed by ssGSEA (single sample Gene Set Enrichment Analysis). Furthermore, we developed six independent, standard algorithms (TIMER, CIBERSORT-ABS, quanTIseq, xCell, TIP, and MCP-counter) to estimate the relative infiltration level of the tumor-infiltrating immune cells (TIICs) in PAAD samples, and it was comprehensively calculated by six independent algorithms to avoid potential calculation errors. The effector TIICs associated genes and 20 co-inhibitory immune checkpoints genes were also evaluated by "ComplexHeatmap" and "corrplot" R software packages, respectively. Finally, the chi-square test was used to compare the distribution of mutation frequencies between each sample set, and the top 15 genes with the highest mutation frequencies were categorized according to ZDHHC3 expression levels.

Immune cell infiltration with the QUANTISEQ algorithm

The R software "ggstatsplot" package was used to explore the relationship between ZDHHC3 gene expression and immune cell infiltration score. Spearman's correlation analysis was used to test for the correlation. *P* values less than 0.01 and 0.05 were considered statistically significant.

Lin *et al. Journal of Translational Medicine*   (2023) 21:249

Page 5 of 24

In vivo Panc 02 pancreatic tumor xenograft mouse models

The ZDHHC3 lentiviral short hairpin RNA (shRNA) vector was designed and purchased from Tsingke (Beijing, China) and was used to construct stable transfection Panc 02 pancreatic cell lines. The PD-L1 overexpressing in ZDHHC3-knockdown Panc 02 cell line was constructed by a recombinant lentivirus (pLV-PD-L1-puro) and performed following the manufacturer's instruction (GENE, China). The shZDHHC3 sequence is 5′-CCC AAAGGAAATGCCACTAAA-3′. Then 5×10^6 (Control, shZDHHC3, shZDHHC3 + PD-L1) Panc 02 cells and their vehicle groups in a volume of 100 μL phosphate-buffered saline (PBS) were injected subcutaneously into the right flank region of 6–8-week-old C57B6/J immunocompetent mice. After the xenografts reached a size around 100–120 mm³, tumor volumes (V) were measured and calculated according to the following equation: $V = 1/2 \times a \times b \times c$ (a, b, c represent the orthogonal axes). Thereafter, 2-BP (0, 50 mg/kg), the palmitoylation inhibitor, was injected peritoneally once per day into mice carrying Panc 02 tumors ($n = 8$ mice per group). Tumor sizes were measured every 3 days. At the last indicated time point, Panc 02 tumors were dissected and cells were mechanically disaggregated using the collagenase type I (400 U/mL; Millipore) for approximately 30 min at 37 °C. After the digestion of tumor tissues, cells were passed through 70-μm filters and collected by centrifugation for further experiments. The wildtype Panc 02 xenograft mouse models were established in a similar manner to verify the synergistic anti-tumor effects of 2-BP in anti-PD-1 or anti-PD-L1 inhibitors. Tumor-bearing mice were treated in the same way with 2-BP (0, 50 mg/kg) ($n = 6$ mice per group), the PD-1 mAb (BE0273, Bio X Cell) or Ig2a isotype control (BE0089, Bio X Cell) and the PD-L1 mAb (BE0101, Bio X Cell) or its isotype vehicle (200 μg per mouse) were intraperitoneally injected every three days according to the treatment plan. Besides, the tumor volume (V) was recorded in the same way. All animals experiments conducted in this study were approved by our Institutional Animal Care Ethics Committee of Wenzhou Medical University.

Cell proliferation assay and in vitro tumorsphere formation assay

All pancreatic cancer cell lines including Panc 02 and PANC-1 cells and human pancreatic ductal epithelial cell line (HPDE6-C7) were purchased from Otwo Biotech Inc (Shenzhen, China). These cell lines were cultured in RPMI 1640 or DMEM supplemented with 10% fetal bovine serum and 1% penicillin/streptomycin (Beyotime, Shanghai, China) at 37 °C in a 5% CO2 atmosphere. All cell lines were authenticated and identified by STR (Short Tandem Repeat) profiling and mycoplasma testing,

respectively. Cell proliferation assay was performed using the Cell Counting Kit-8 (CCK-8, Dojindo, Kumamoto, Japan) assay as previously described [36]. Briefly, twenty-four hours after 2-BP treatment, the Panc 02, PANC-1, and HPDE6-C7 cells were seeded into 96-well culture plates at 2000 cells per well, in triplicate, and incubated overnight. Cells were exchanged for serum-free medium at the indicated time points, 10 μL of the CCK-8 solution was added to each well, and incubated in a humidified incubator for 2 h. Finally, the optical density (OD) at 450 nm was measured immediately using a Versa Max microplate reader. The cell viability rate was calculated as follows: Cell viability (%) = $(OD_{treated} - OD_{blank})/(OD_{control} - OD_{blank}) \times 100\%$.

To silence ZDHHC3 expression in PANC-1 cells, small interfering RNA (siRNA) targeting human ZDHHC3 (si-ZDHHC3) oligos and non-silencing siRNA (si-Control) were constructed and purchased from Tsingke Biological Technology Company (Beijing, China). The sequences (5′-3′) were as follows: si-ZDHHC3#1: CCACAGUGA UUCUCCUUAUTT (sense) and AUAAGGAGAAUC ACUCUGGTT (anti-sense); si-ZDHHC3#2: CCUCAA ACUGGAUUCACUUTT (sense) and AAGUGAAUC CACUUUGAGGTT (anti-sense). SiRNA transfection was done using the Fugene transfection reagent (Roche, Basel, Switzerland) following the manufacturer's instructions.

For the tumorsphere formation assay, tumorsphere growth medium was freshly prepared by containing 500 mL of Dulbecco's Modified Eagle Medium/F12 with B27 supplement (final concentration, $1 \times$), epidermal growth factor (final concentration, 20 ng/mL), basic fibroblast growth factor (final concentration, 10 ng/mL), 0.4% Bovine Serum Albumin), and penicillin/streptomycin. 4000 cells per well of 6-well plate suspended in the tumor sphere medium and the cells were then incubated for an additional 7 days, then the primary sphere number was counted under a phase-contrast microscope at $40 \times$ magnification.

Cell apoptosis, cell migration, and cell-cycle analysis

Assessment of cell apoptosis was performed using the cell apoptosis detection kit (Annexin V-FITC/PI, Dojindo) as previously described [37]. Briefly, Panc 02, PANC-1, and HPDE6-C7 cells were seeded into 24-well plates with 500 μL of culture medium at an initial density of 50,000 cells per well. After co-incubating with 2-BP or DMSO at different concentrations for the indicated time, cell apoptosis was constructed as manufacturer's instruction and detected using the BD Accuri C6 flow cytometer (BD Sciences, USA).

For wound-healing assay, cells were treated with 2-BP as before. The cell resuspension at 3×10^5 cells/mL was

Lin *et al. Journal of Translational Medicine*   (2023) 21:249

Page 6 of 24

added into the chamber of the μ-dish (Ibidi, Munich, Germany). Thereafter, the inserts were slowly removed until the cells adhered to the μ-dish wall and incubated in serum-free medium at 37 °C and 5% CO_2. A microscope was performed to take images at 0 h and 24 h. The rate of migration was computed with ImageJ software. Cell-cycle analysis was performed as described previously [26].

Immunohistochemical staining and enzyme-linked immunosorbent assay (ELISA)

For immunohistochemical staining of Panc 02 tumor tissues, the xenograft tumor tissues were formalin-fixed and paraffin-embedded for subsequent immunohistochemical staining. Paraffin sections were routinely deparaffinized in xylene and rehydrated in a graded series of ethanol. Heat antigen retrieval was performed by microwaving in sodium citrate buffer (pH 6.0). Then, endogenous peroxidase in tissue sections was quenched with a 3% H_2O_2 in methanol for 15 min. Subsequently, tumor tissue sections were blocked in 10% normal horse serum and 0.3% triton X-100 for 1 h, then incubated with the indicated primary antibody diluted in 2.5% normal horse serum blocking solution: The used primary antibody: PD-L1 (13684, Cell Signaling Technology), CD8 (98941, Cell Signaling Technology), and Granzyme B (46890, Cell Signaling Technology). After incubation with the specific primary antibody overnight, sections were incubated with the Vectastain ABC Elite kit (Vector Labs, Burlingame, CA, USA). Slides were viewed and photomicrographs were captured under a light microscope (Olympus, Japan).

Samples of Panc 02 cells were treated with or without 2-BP (100 μM) for 24 h. The cell supernatant from each culture was collected for the assay. The concentrations of CCL4, CCL5, CXCL9 and CXCL10 in these supernatants and tumor tissues of Panc 02 xenografts were determined by ELISA kits from R&D Systems following the manufacturer's protocol.

Immunoblotting, co-immunoprecipitation (co-IP), and real-time quantitative PCR (RT-qPCR)

For immunoblotting, tumor cells were lysed in RIPA buffer (Beyotime, China) and pelleted of the insoluble material via centrifugation. The protein concentration was determined using a BCA protein assay kit (Beyotime, China). The protein samples, at equal concentrations, were separated with SDS-PAGE using 10% gels, and the protein bands were then transferred onto polyvinylidene fluoride (PVDF) membranes (Millipore, USA). Following blocking the membrane with 5% nonfat milk TBST buffer at room temperature for 1.5 h, the primary antibody was subsequently incubated with it at

4 °C overnight. Washing with $1 \times$ TBST for 3 times, the membrane and the appropriate concentrations of secondary antibody were then co-incubated in RT for 1 h. Finally, the ECL detection reagents (Beyotime, China) were reacted with PVDF membranes and imaged by X-ray exposure. For immunoblotting, the antibodies were used at the indicated dilutions according to the manufacturer's recommendations. ZDHHC3 (ab31837, Abcam), NANOG (14295-1-AP, Proteintech), SOX2 (11064-1-AP, Proteintech), OCT4 (11263-1-AP, Proteintech), ALDH1 (15910-1-AP, Proteintech), PD-L1 (13684, Cell Signaling Technology), mTOR (2983, Cell Signaling Technology), Phospho-mTOR (5536, Cell Signaling Technology), β-actin (66009-1-Ig, Proteintech).

Co-IP experiments were performed to investigate the ZDHHC3 and PD-L1 protein interactions. Briefly, PANC-1 cells were lysed by IP buffer (P0013J, Beyotime) and centrifuged to obtain the supernatants, then primary antibody and agarose beads were added subsequently for the incubation at 4. After washing 4 times with PBST (0.03% Tween-20 in PBS), samples were reconstituted in 2× sodium dodecyl sulfate–polyacrylamide gel electrophoresis buffer and boiled at 90 °C for 10 min. Then samples were subjected to electrophoresis with 10% gel and analyzed by immunoblotting with indicated antibodies.

RT-qPCR assay was performed to detect PD-L1 mRNA level in ZDHHC3 knockdown PANC-1 cells. siRNA targeting ZDHHC3 and siRNA negative control (siControl) were synthesized by Beijing TSINGKE Biological Technology Co. Ltd. The sequences of siControl were: sense strand, 5′-UUCUCCGAACGUGUCACGUTT-3′, antisense strand, 5′-ACGUGACACGUUCGGAGAATT-3′. PANC-1 cells were treated with si-ZDHHC3 or si-Control for 48 h. Then, cells were harvested, and total RNA was extracted. The subsequent procedures were consistent with those in our previous study [37]. PD-L1 forward primer (5′-GCTATGGTGGTGCCGACTAC-3′), PD-L1 reverse primer (5′-TGGCTCCCAGAATTACCAAGT-3′); GAPDH forward primer (5′-CGCTCTCTGCTCCTC CTGTTC-3′) GAPDH reverse primer (5′-ATCCGTTGA CTCCGACCTTCAC-3′).

Immunofluorescence and flow cytometry analysis

Immunofluorescence (IF) staining and confocal microscopy was performed to determine protein colocalization of ZDHHC3 and PD-L1 on PANC-1 cells. After fixing in 4% paraformaldehyde for 15 min, PANC-1 cells were permeated and blocked with 1% BSA and 0.2% Triton X100 for 1 h at room temperature (RT). PANC-1 Cells were then incubated with the indicated primary antibody overnight at 4 °C. Following 3 washes in PBS, the fluorescently conjugated secondary antibodies were applied (Invitrogen, 1:1000) and co-cultured with the cells for

Lin *et al. Journal of Translational Medicine*   (2023) 21:249

Page 7 of 24

30 min at RT. Slides were mounted prolong gold anti-fade reagent with DAPI (Invitrogen, USA) after being washed with PBS for 3 times and imaged on an LSM880 confocal microscope (ZEISS, Germany).

For flow cytometry analysis of tumor tissues, The isolated cells obtained from Panc 02 xenografts in mice, were stained with Fixable Viability Dye eFluor™ 455UV (eBioscience) and stained with a mixture of fluorochrome-conjugated antibodies: CD45-FITC (Biolegend, 553079); CD3-BB700 (BD Pharmingen, 566494); CD4-APC (eBioscience, 17-0042-82); CD8-PE (eBioscience, 12-0081-82); CD11b-FITC (Biolegend, 557396); CD11c-PerCP-Cy™5.5 (BD Pharmingen, 560584); CD206-PE-Cy7 (eBioscience, 2349850); and F4/80-BV421 (BD Pharmingen, 565411). Anti-human-PD-L1-APC (329707; BioLegend) was used to detect the expression of PD-L1 on PANC-1 cancer cells. Data were acquired on an Attune NxT flow cytometer (Thermo Fisher). Compensation and data analysis were performed by FCS Express 10.0 software. The baseline gate was adapted by the controls containing unstained and single-color biological controls, while a sequential gating strategy was used to identify immune cell subsets.

Statistical analysis

Data are expressed as means ± standard deviation (SD) or means ± standard error (SEM). Two groups were compared using a two-tailed unpaired Student's t test or Mann–Whitney U test. More than two groups were analyzed by using one-way ANOVA followed by Tukey's multiple comparison tests. Statistics were calculated using GraphPad Prism software V5 (GraphPad Software Inc., San Diego, CA, USA). Statistically significant differences were considered significant when *$p < 0.05$, **$p < 0.01$, and ***$p < 0.001$.

Results

Identification of pancreatic cancer-related ZDHHC enzymes

To date, ZDHHC family members of the palmitoyl transferase have been shown to interact with their corresponding tumor-associated substrate proteins, thus closely linked with tumor initiation and malignant progression. Given the fact that their role in the tumorigenic

ability of pancreatic cancer is variable, we speculated that the characterization of key ZDHHC family genes involved in PAAD would provide potential pancreatic cancer driver genes and therapeutic targets for the treatment of pancreatic cancer. To clarify the expression of ZDHHCs in PAAD, we first used RNA-seq data from the TCGA database to evaluate the expression levels of ZDHHC family members between adjacent normal pancreas tissues and pancreatic cancer tissues. As shown in Fig. 1A, after including the normal cases from GTEx project as controls, the expression level of 11 ZDHHCs (ZDHHC3/4/5/6/7/9/12/14/16/18/20) were significantly elevated in PAAD tissues compared with adjacent normal tissues ($P < 0.05$) and we did not obtain significant expression difference of other ZDHHCs. Meanwhile, we used the Human Protein Atlas (HPA) database to further investigate the protein levels of ZDHHC family members in PAAD. The levels of ZDHHCs staining were classified as high, medium, low, and not detected based on immunohistochemical staining intensity results. In all, the protein levels of ZDHHC 1/3/4/5/7/9/12/17/20/21/24 were increased in PAAD tissues (Fig. 1B; Additional file 1: Fig. S1). However, ZDHHC19 and ZDHHC22 were not detected. Additionally, we analyzed the relationship between individual cancer stages of PAAD patients with the mRNA expression patterns of different ZDHHC family members by GEPIA database. The results suggested that high ZDHHC3/4/7/9/15/17/20/22 expression in pancreatic cancer is closely related to patients' individual cancer stages, and advanced cancer patients were more inclined to express higher mRNA expression of ZDHHC3/4/7/9/15/17/20/22 (all $P < 0.05$) (Additional file 1: Fig. S2), and other ZDHHCs show no significant difference (Additional file 1: Fig. S3). Furthermore, we separated the pancreatic cancer patients into high- and low-expression groups based on the median value of ZDHHCs expression, and then explored the association between 23 ZDHHCs expression levels and the clinical prognosis of PAAD patients by the Kaplan–Meier plotter database. As displayed in (Fig. 1C; Additional file 1: Fig. S4), high expression of ZDHHC3/5/9/18/20 and low expression of ZDHHC1/8/11/14/15/17/21/22/24 was related to poorer prognosis of overall survival (OS). High expression of ZDHHC3/4/5/7/9/20 and low expression of

(See figure on next page.)

Fig. 1 Expression profiles and survival analysis of ZDHHC genes in PAAD tumors. **A** The GEPIA database analysis revealed the ZDHHCs expression in pancreatic cancer tissues versus normal pancreatic tissues. The ZDHHCs expression levels were expressed in log2 (TPM + 1) log scale (TPM: transcript per million). Statistical differences between pairs of groups were determined using Student's t-test and the p-value cutoff was 0.05. The red font represents up-regulation, and the black font represents no expression difference. **B** The protein expression of different ZDHHCs in PAAD is summarized based on the immunohistochemistry results of the Human Protein Atlas (HPA) database. **C** Univariate and multivariate Cox regression analysis of (OS/RFS) based on ZDHHCs expression in TCGA-PAAD cohort. Each horizontal line represents the 95% confidence interval (CI). The vertical dotted line indicates HR = 1. HR exceeding 1.0 indicates ZDHHCs overexpression is an unfavorable and independent prognostic factor in PAAD patients (*$p < 0.05$)
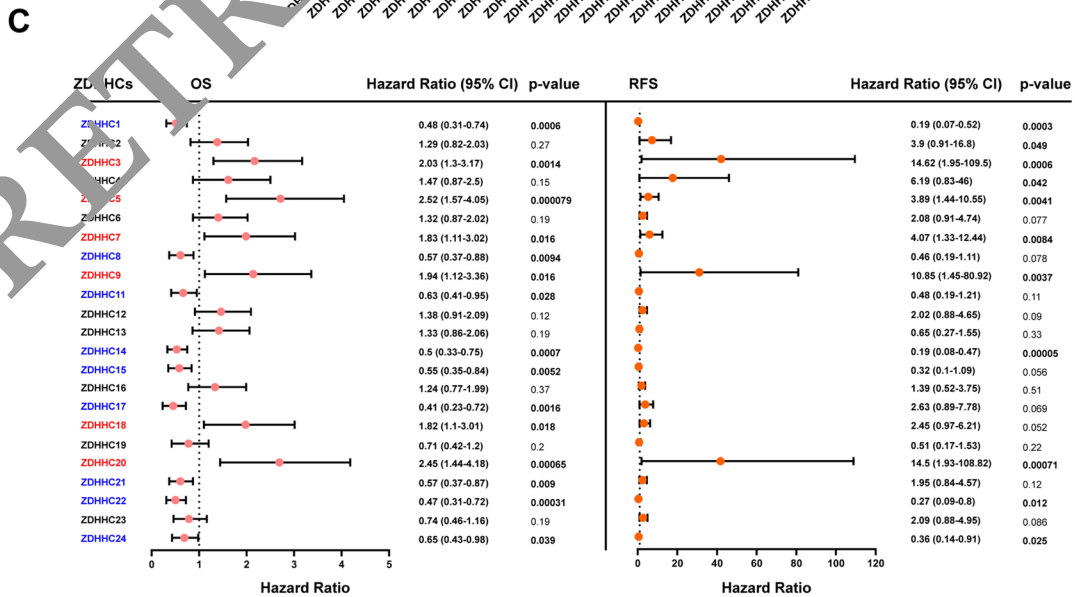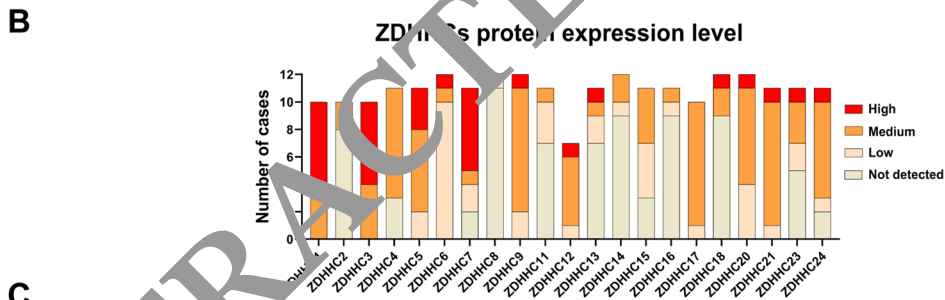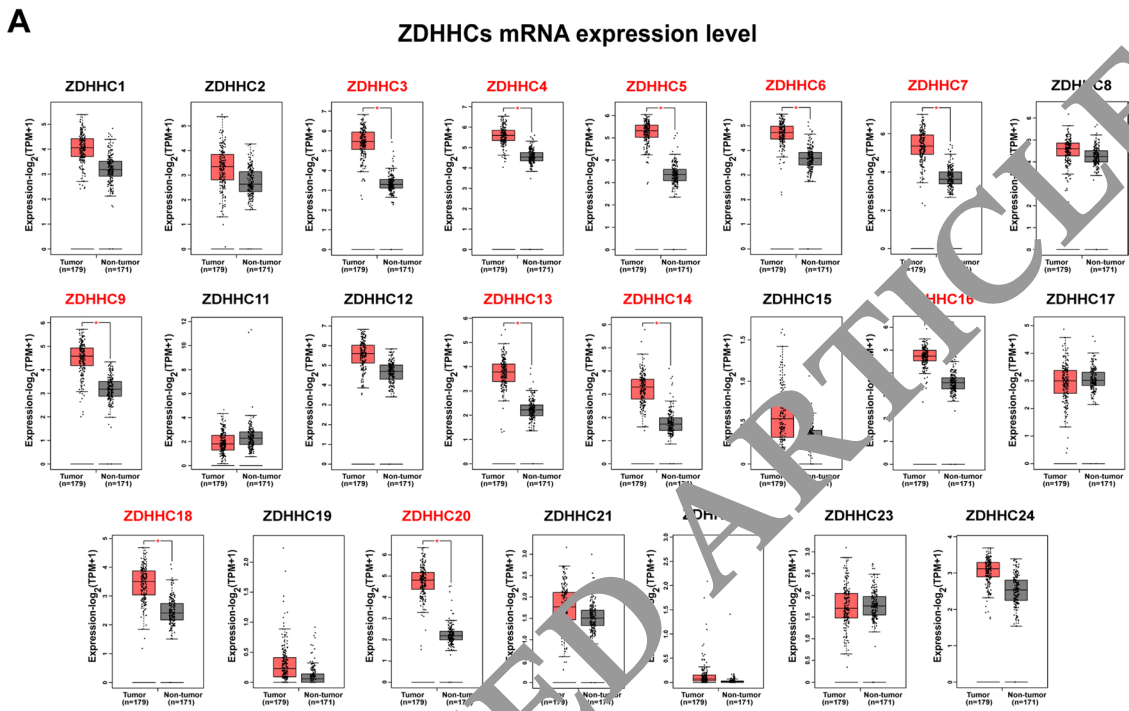
Fig. 1 (See legend on previous page.)

Lin *et al. Journal of Translational Medicine*   (2023) 21:249

Page 9 of 24

ZDHHC1/14/22/24 were related to poorer prognosis of relapse-free survival (RFS). Taken together, ZDHHC3/9 are the only two ZDHHC enzymes with statistically differential expression patterns, pathological stages, and prognostic values in PAAD.

Pan-cancer expression pattern, prognostic value, and immunological infiltration correlation of ZDHHC3

Based on the expression level of ZDHHC3 was selectively elevated in PAAD among 33 pan-cancers according to the GEPIA database (Fig. 2A), we further analyzed the expression of ZDHHC3 in PAAD. The mRNA level of ZDHHC3 in PAAD tissues with that in corresponding adjacent normal tissues were compared using 2 independent studies from the GEO database. As shown in Fig. 2B, ZDHHC3 mRNA expression level was also markedly upregulated in PAAD patients' tissues. ($P < 0.001$). To clarify that ZDHHC3 was similarly elevated at the protein level in PAAD patients' tissues, we checked the CPTAC dataset using the UALCAN portal. Indeed, in the CPTAC dataset, ZDHHC3 protein expression was upregulated, regardless of the clinicopathological characteristics of patients, including cancer stage and tumor grade (Fig. 2C). Furthermore, immunohistochemical staining results of ZDHHC3 in PAAD and normal pancreatic tissue were obtained from the HPA database (Fig. 2D). We found that 6 out of 10 pancreatic cancer tissues, including that of patient ID 3614/1394/779, showed a markedly high ZDHHC3 staining level and 4 out of 10 pancreatic cancer tissues, including that of patient ID 3363/1098/3233, showed a medium ZDHHC3 staining level. Basic annotation parameters were determined visually from HPA image by pathologists. ZDHHC3 was positively stained in >75% of tumor cells in a high proportion of cases, with the medium and high staining scores in PAAD. In pancreas normal tissues, ZDHHC3 showed medium-staining intensity in 25–75% of exocrine glandular cells and low-staining intensity in 25–75% of pancreatic endocrine cells. Next, we assessed the relationship between the ZDHHC3 expression and the prognosis of patients across the pan-cancer dataset. The OS and disease-specific survival (DSS) were analyzed for all included patients. Pan-cancer results of cox regression analysis indicated that the ZDHHC3 expression significantly negatively correlated with OS in 6 types of cancer including PAAD, acute myeloid leukemia (LAML), liver hepatocellular carcinoma (LIHC), skin cutaneous melanoma (SKCM), and mesothelioma (MESO) (Additional file 1: Fig. S5). The increased ZDHHC3 expression corresponded with poor DSS in patients with PAAD and SKCM (Additional file 1: Fig. S6). Collectively, these results suggest that ZDHHC3 might serve as a novel

prognostic biomarker and exert a tumor-promoting property in pancreatic cancer.

ZDHHC3 expression promotes an immunosuppressive tumor microenvironment

Previous studies have reported ZDHHC3 in colon cancer as a main palmitoyl transferase of PD-L1 to inhibit anti-tumor response [23]. However, the biological role of ZDHHC3 in the immune status of TME and whether it affects immune cell infiltration is unclear. Baseline T cell infiltration within the tumor microenvironment can predict and influence the effect of tumor immunotherapy [38]. Mark Ayers and colleagues established an 18-gene expression signature to assess pre-existing adaptive T cell immune responses [39]. As shown in Fig. 3A, B, ZDHHC3 expression was significantly negatively correlated with the pan-cancer T cell infiltration score (R = −0.2, *r* = 0.01), indicating that ZDHHC3 is a potent immunosuppressive molecule. Next, we further demonstrated the potential immunomodulatory roles of ZDHHC3 in different tumor types to identify candidate types that may benefit from ZDHHC3-targeted therapy. Our findings showed that ZDHHC3 was found to be negatively correlated with a majority of immunomodulators in PAAD (Fig. 3C), the established gene signature of the pro-inflammatory TME [40]. We also investigated the infiltration levels of TIICs using the TISIDB database. Furthermore, ZDHHC3 expression was mutually exclusive of four immune checkpoints, including PD-1, cytotoxic T lymphocyte antigen 4 (CTLA-4), and lymphocyte activation gene 3 (LAG-3) expression in some cancer types, including PAAD (Fig. 3D–G). We further noted that ZDHHC3 was negatively associated with TMB (Tumor mutational burden) and MSI (Microsatellite instability) in several cancer types (Additional file 1: Fig. S7). Notably, ZDHHC3 expression was negatively correlated with a majority of immune cells in some cancer types, including PAAD (Fig. 3H). Together, these results indicate that ZDHHC3 may be used as a potential indicator of tumor immunogenicity in some human cancers.

We next focused on the immunomodulation of ZDHHC3 in pancreatic cancer. Of these, a majority of MHC protein complex related genes were downregulated in the high-ZDHHC3 group, suggesting a possible impairment of the antigen uptake, processing, and presentation compared to low-ZDHHC3 group. Notably, chemokines including (CCL4, CCL5, and CXCL9), identified to be critical for recruitment of activated CD8$^+$ T cells into the TME, were also downregulated in the high-ZDHHC3 group. Similarly, other chemokines, including CCL2, CCL3, CCL8, CCL11, CCL12, CCL14, CCL16, CCL19, CCL21, and CCL23, and paired receptors including CCR1, CCR2, CCR4, CCR5, CCR6, CCR7, CXCR1,
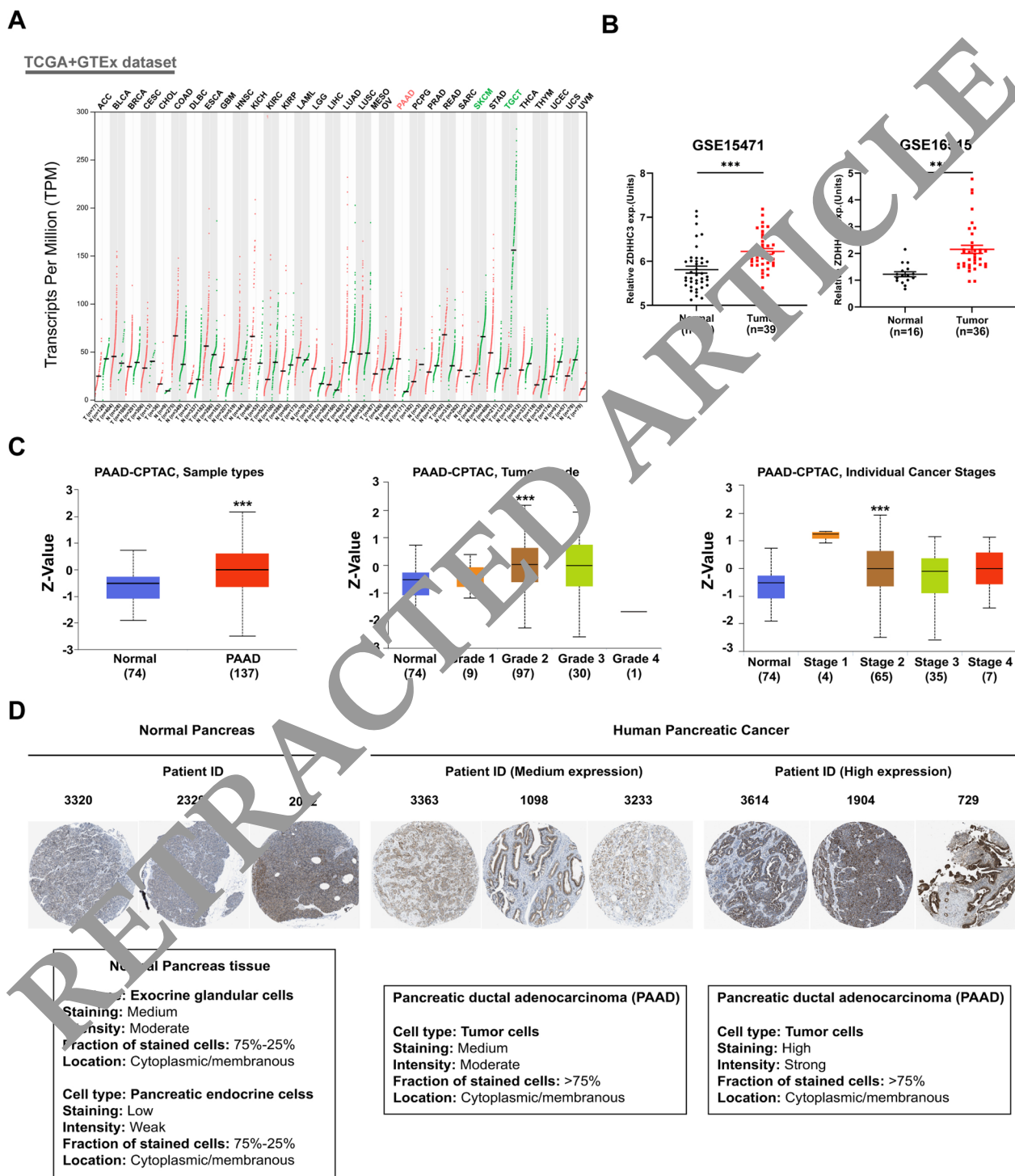
Fig. 2 Expression of ZDHHC3 in human pancreatic cancer and adjacent normal pancreatic tissues. **A** Expression of ZDHHC3 in tumor and normal tissues in pan-cancer data from the TCGA and GTEx database using GEPIA database. **B** Differential expression profile of ZDHHC3 in paired pancreatic tumor and adjacent normal tissues from the GEO database. **C** Box-plot analysis represents the protein expression level of ZDHHC3 in PAAD and normal pancreatic tissues through the UALCAN web server. The raw proteomic data are available via the CPTAC data portal, including the tumor grade, and cancer stage. **D** Representative images of immunohistochemistry for ZDHHC3 in PAAD tissues. The histological subtypes were used to address the heterogeneity of PAAD and normal pancreas tissues based on the ZDHHC3 expression

Lin *et al. Journal of Translational Medicine*   (2023) 21:249

Page 11 of 24

and CXCR6, were found to be negatively correlated with ZDHHC3 expression in PAAD (Fig. 4A; Additional file 1: Fig. S8). These chemokines and receptors are known to orchestrate the traffic of effector TIICs such as NK cells, CD8$^+$ T cells, and antigen-presenting cells to the tumor site, can in turn initiate anti-tumor immunity. A series of stepwise anti-tumor immune response events has been previously established to dissect the complex cancer-immune system interactions [41]. The activities of the majority of the steps in the cancer-immunity cycle were suppressed in the high-ZDHHC3 group, including the release of cancer antigens presentation (Step 2), priming and activation (Step 3), and trafficking of immune cells to tumors (Step 4) (CD4$^+$ T cell recruiting, CD8$^+$ T cell recruiting, dendritic cells (DC) recruiting, macrophage recruiting, monocyte recruiting, NK cell recruiting, TH17 recruiting, and B cell recruiting,) (Fig. 4B). Thus, the decreased activities of these key steps may impede the infiltration of effector immune cells into the tumor bed. We next examined the infiltration level of TIICs using six different independent algorithms [42]. Consistent with the above analysis, expression level of ZDHHC3 was negatively associated with the infiltration of CD4$^+$ T cells, NK cells, macrophages, and DCs in different independent algorithms among PAAD samples (Fig. 4C). Similarly, the majority of these TIICs related effector genes were negatively correlated with ZDHHC3 gene expression (Fig. 4D). Low immune checkpoint inhibitors such as PD-L1/PD-1 expression was one of the most notable features in non-inflamed TME of pancreatic cancer [43]. Of note, ZDHHC3 expression was negatively correlated with a majority of immune checkpoints including PD-1, CTLA-4, LAG-3, TIM-3, TIGIT, CD200, and ADORA2A (Fig. 4E). In summary, ZDHHC3 overexpression may exert an immune suppressed effect in pancreatic cancer.

Mutation landscape between ZDHHC3-high and ZDHHC3-low pancreatic tumors

PAAD patients with KRAS mutation, TP53 mutation, and CDKN2A mutation were more likely to have faster disease progression and worse clinical outcome [44]. We further evaluated the mutation status among the ZDHHC3-high and ZDHHC3-low groups of TCGA-PAAD cohort. Among these altered genes, TP53, KRAS, and CDKN2A
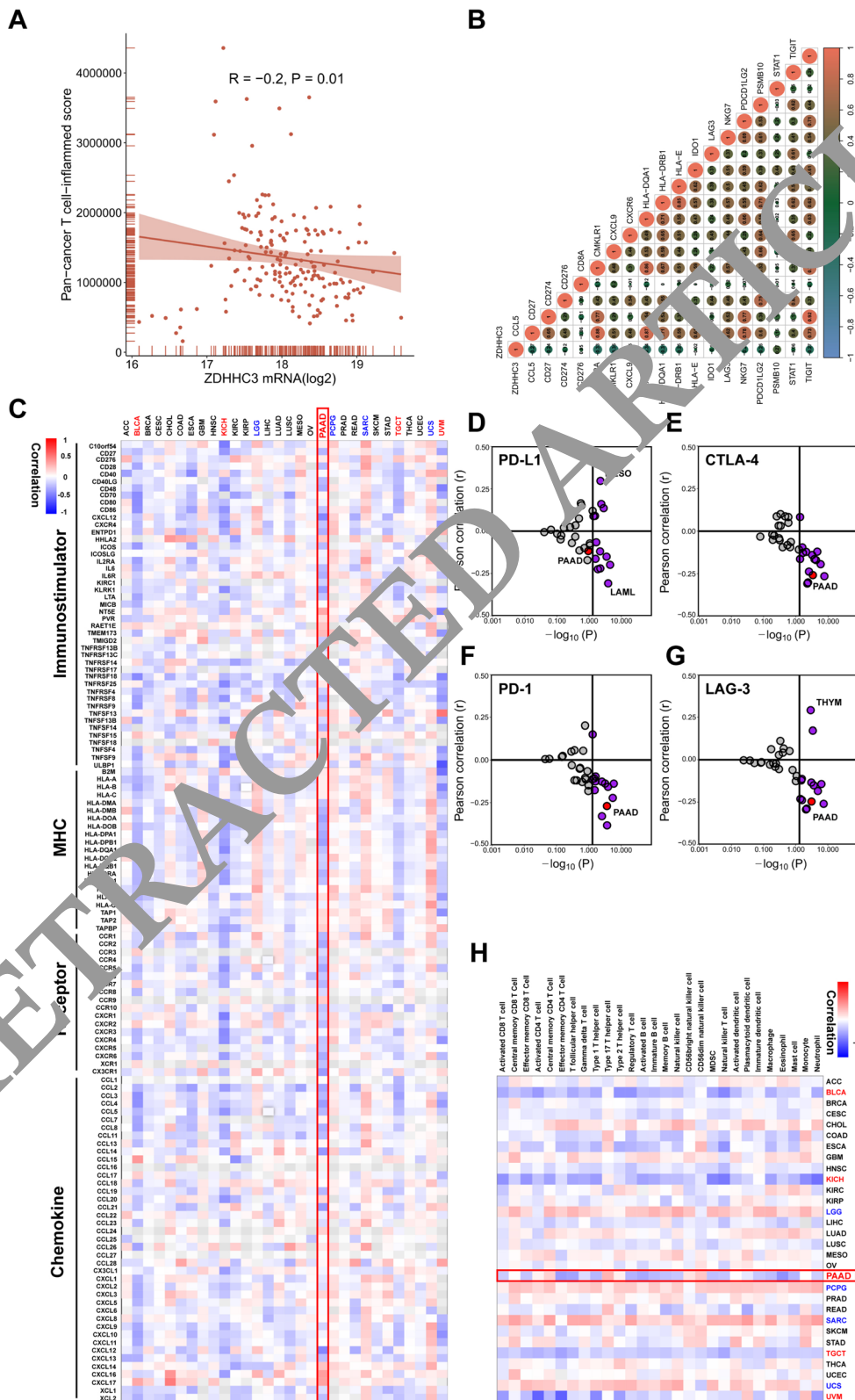
were the most significantly differentially mutant genes (Fig. 5A, B). ZDHHC3-high tumors were found to harbor a higher prevalence of TP53 and KRAS mutation rate, indicating the enhanced tumorigenic potential (Fig. 5A, B). Likewise, as ZDHHC3 expression increased, the frequency of KRAS and TP53 gene mutations increased (Additional file 1: Fig. S9). Meanwhile, when compared to wild type KRAS PAAD samples (27%, 17/63), tumors with high KRAS mutation rate samples were more likely to be ZDHHC3-high (70%, 56/80). Meanwhile, when compared to wild type TP53 PAAD samples (32%, 26/80), tumors with TP53 mutation were more likely to express higher ZDHHC3 level (75%, 47/63) (Fig. 5C, D). Moreover, the GSEA results and KEGG analysis indicated that ZDHHC3 is significantly positively associated with the mutant TP53-upregulated genes, while negatively correlated with the mutant TP53-downregulated genes (Fig. 5E, F; Additional file 1: Fig. S10). Furthermore, we found that PAAD patients with p53 induced genes had low ZDHHC3 expression, while the PAAD patients with p53 suppressed genes had higher ZDHHC3 expression (Fig. 5G). Taken together, these results demonstrate that ZDHHC3-high tumors harbor a higher TP53 and KRAS mutation rate, which may cooperatively contribute to disease progression and prognosis status in pancreatic cancer.

ZDHHC3 knockdown slows Panc 02 tumor growth with enhanced anti-tumor immunity

Based on the above results, we hypothesized that ZDHHC3 may promote the development and progression of pancreatic cancer. We next tested the role of ZDHHC3 on oncogenic phenotypes using the Panc 02 syngeneic pancreatic cancer model. Stable knockdown of ZDHHC3 in Panc 02 cells was achieved using the shRNA approach (shZDHHC3). Knockdown efficiency of endogenous ZDHHC3 was assessed by western blotting analysis (Fig. 6A). We transplanted control (shControl) or ZDHHC3 knockdown (shZDHHC3) Panc 02 cells subcutaneously into the right flank of immunocompetent mice and the local volume changes in tumor growth were monitored every 3 days. We observed that genetic inactivation of ZDHHC3 slowed tumor growth and decreased the final tumor burden when compared to

(See figure on next page.)

Fig. 3 Correlation among ZDHHC3 gene expression and immunological status in pan-cancer analysis. **A**, **B** Pan-cancer analysis of correlations between ZDHHC3 gene expression and T cell inflamed score (**A**) and the 18 individual component genes from the established T cell inflamed signature (**B**). The T cell inflamed score is significantly positively correlated with immunotherapy response in cancer. **C** Heat map images show the correlation between ZDHHC3 gene expression and 124 immunomodulators such as MHC, immunostimulator, chemokine, and chemokine receptors using the TISIDB database. **D–G** Correlation between ZDHHC3 gene expression and four immune checkpoints, PD-L1 (**D**), CTLA-4 (**E**), PD-1 (**F**), and LAG-3 (**G**). The different color dots represent different cancer types. The Y-axis indicates the Pearson correlation coefficient and the X-axis indicates -log$_{10}$P values. **H** Heat map images show the correlation between ZDHHC3 gene expression and 28 tumor-infiltrating immune cells in the TME. The heat map color indicates the correlation coefficient. Red color, positive correlations; blue color, negative correlations. The horizontal axis indicates the infiltration levels of immune cells, and the vertical axis indicates the different cancer types

Fig. 3 (See legend on previous page.)

Lin *et al. Journal of Translational Medicine* (2023) 21:249

Page 13 of 24

shControl Panc 02 tumors, thus prolonging the survival time of Panc 02 tumor bearing mice (Fig. 6B–D). Data from human pancreatic cancer suggest a potential function for ZDHHC3 in shaping the non-inflamed pancreatic cancer tumor microenvironment. We next assessed whether the ZDHHC3-dependent antitumor activity was associated with the potentiation of an adaptive antitumor immune response, similar to the above results that ZDHHC3 expression promotes an immunosuppressive TME in human pancreatic cancer. Panc 02 tumor samples were analyzed by multicolor flow cytometric analysis. A significant increase in the infiltration levels of anticancer immune cells, including NK cells, CD4^{+} and CD8^{+} T cells, DCs, and M1 macrophages in ZDHHC3-knockdown Panc 02 tumors as compared to shControl Panc 02 tumors. No significant difference in the infiltration of M2 macrophages was observed in shZDHHC3 Panc 02 tumors compared to shControl Panc 02 tumors (Fig. 6E–H). Since ZDHHC3 knockdown (KD) induced a characteristic immune profile in Panc 02 tumors, we hypothesized that ZDHHC3 knockdown would lead to a change in the cytokine/chemokine profile of the tumor microenvironment. To test this hypothesis, we used ELISA approach to detect the expression amounts of CCL4, CCL5, CXCL9, and CXCL10 in ZDHHC3-knockdown Panc 02 tumor tissues. CXCL9 protein showed the greatest increase in expression in response to ZDHHC3-KD (3.7-fold versus shControl). Meanwhile, CCL5 and CXCL10 protein increased by 1.5 times in response to ZDHHC3-KD, respectively and we did not detect significant changes in CCL4 expression (Additional file 1: Fig. S11). CXCL9 has been identified as the critical chemokine which recruit immune cells that express its cognate receptor, CXC-chemokine receptor 3 (CXCR3), including activated T cells and NK cells [45]. Meanwhile, the dendritic cells (DC) score was also highly correlated with CXCL9 mRNA levels and previous studies have reported that DCs secrete CXCL9 and thereby contribute to the recruitment of CD8^{+} T cells and NK cells [45]. Based on our results that a significant increase in the infiltration levels of anticancer immune cells, including NK cells, CD8^{+} T cells, and DCs in ZDHHC3-knockdown Panc 02 tumors as compared to shControl Panc 02 tumors, it would be very interesting to identify whether

the functional role of ZDHCH3 in regulating anti-tumor immunity was CXCL9 mediated in future study.

We next explored potential key molecular targets for the inhibition of pancreatic cancer growth after knockdown of ZDHHC3. Previous studies have shown that ZDHHC3 palmitoylates PD-L1 to maintain its protein stability in colon cancer and gliomas [23, 46]. We next sought to determine whether ZDHHC3 influences cancer immunity by regulating PD-L1 expression in pancreatic cancer cells. Accordingly, we knockdown endogenous ZDHHC3 using two independent siRNAs in PANC-1 cells and detected PD-L1 expression. As shown in (Additional file 1: Fig. S12A, B), ZDHHC3 knockdown decreased PD-L1 protein expression, while not affecting its mRNA expression. These results were consistent with decreased surface expression of PD-L1 on ZDHHC3 knockdown PANC-1 cells (Additional file 1: Fig. S12C, D). Since palmitoyl transferases are known to interact with their substrates, we next investigated whether ZDHHC3 binds to PD-L1 in PANC-1 cells. Double immunofluorescent staining demonstrated that endogenous ZDHHC3 colocalized with PD-L1 in cultured PANC-1 cells (Additional file 1: Fig. S12E, F). Meanwhile, co-immunoprecipitation indicated physical interactions between PD-L1 and ZDHHC3 that were expressed endogenously in PANC-1 cells (Additional file 1: Fig. S12G). Thus, our findings indicated that ZDHHC3 is a key palmitoyl transferase to stabilize PD-L1 protein expression in pancreatic cancer, suggesting that the ZDHHC3-high tumors may have T cell exhaustion which contribute to immune evasion. Next, we performed animal assays to further investigate the functioning axis between ZDHHC3 and PD-L1. We introduced ZDHHC3-knockdown with PD-L1 overexpression clones (shZDHHC3 + PD-L1) by lentivirus expression system. Western blotting results revealed that PD-L1 expression is reduced in shZDHHC3 Panc 02 cells and successfully overexpression of PD-L1 expression in (shZDHHC3 + PD-L1) Panc 02 cells (Fig. 6I). We next subcutaneously transplanted control, ZDHHC3-knockdown, and ZDHHC3-knockdown with PD-L1 overexpressed Panc 02 cells into the right flank of immunocompetent mice and observed tumor growth. Overexpression of PD-L1 can almost

(See figure on next page.)

Fig. 4 ZDHHC3 expression promotes an immunosuppressive TME in PAAD. **A** Heat map showing different expression levels of published immunomodulators signatures (MHC, immunostimulator, chemokine, and chemokine receptors) between high- and low-ZDHHC3 groups in PAAD patients. **B** The expression patterns of markers of anti-cancer immunity across a 7-step cancer-immunity cycle between high- and low-ZDHHC3 groups. **C** The association between ZDHHC3 gene and the infiltration degrees of five TIICs (CD8^{+} T cells, NK cells, macrophages, Th1 cells, and DC), based on different algorithms. **D** A differential heat map showing the comparison of the published effector gene profiles of indicated immune cells between high and low ZDHHC3 groups. The heat map color indicates the correlation coefficient. Yellow color, positive correlations; blue color, negative correlations. **E** Correlation between ZDHHC3 gene expression and 20 inhibitory immune checkpoints in PAAD samples. Color scales visualizes Spearman correlation coefficient values. Color codes in the heat map represent relative expression levels as z-scores. *P*-values were calculated using Mann–Whitney U test with asterisks (*$p < 0.05$, **$p < 0.01$, ***$p < 0.001$, and ****$p < 0.0001$)

Lin *et al. Journal of Translational Medicine*   (2023) 21:249
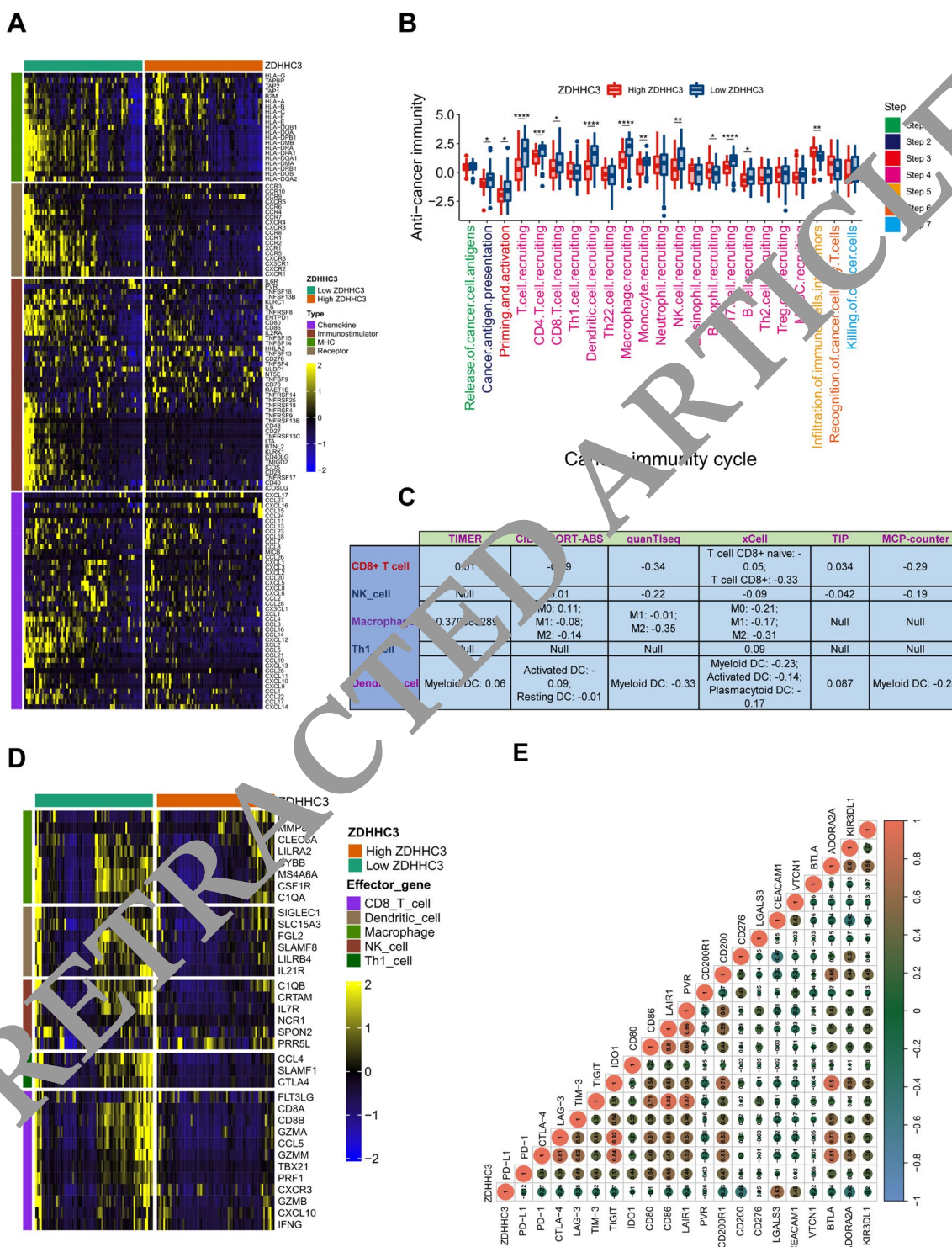
Page 14 of 24

Fig. 4 (See legend on previous page.)

completely reverse ZDHHC3 knockdown-induced inhibition of Panc 02 tumor growth and prolongation of mice survival time (Fig. 6J–L), suggesting that ZDHHC3 promotes pancreatic cancer progression

probably via upregulation of PD-L1 expression by palmitoylation. Taken together, combining comprehensive bioinformatics and preclinical animal model results, we
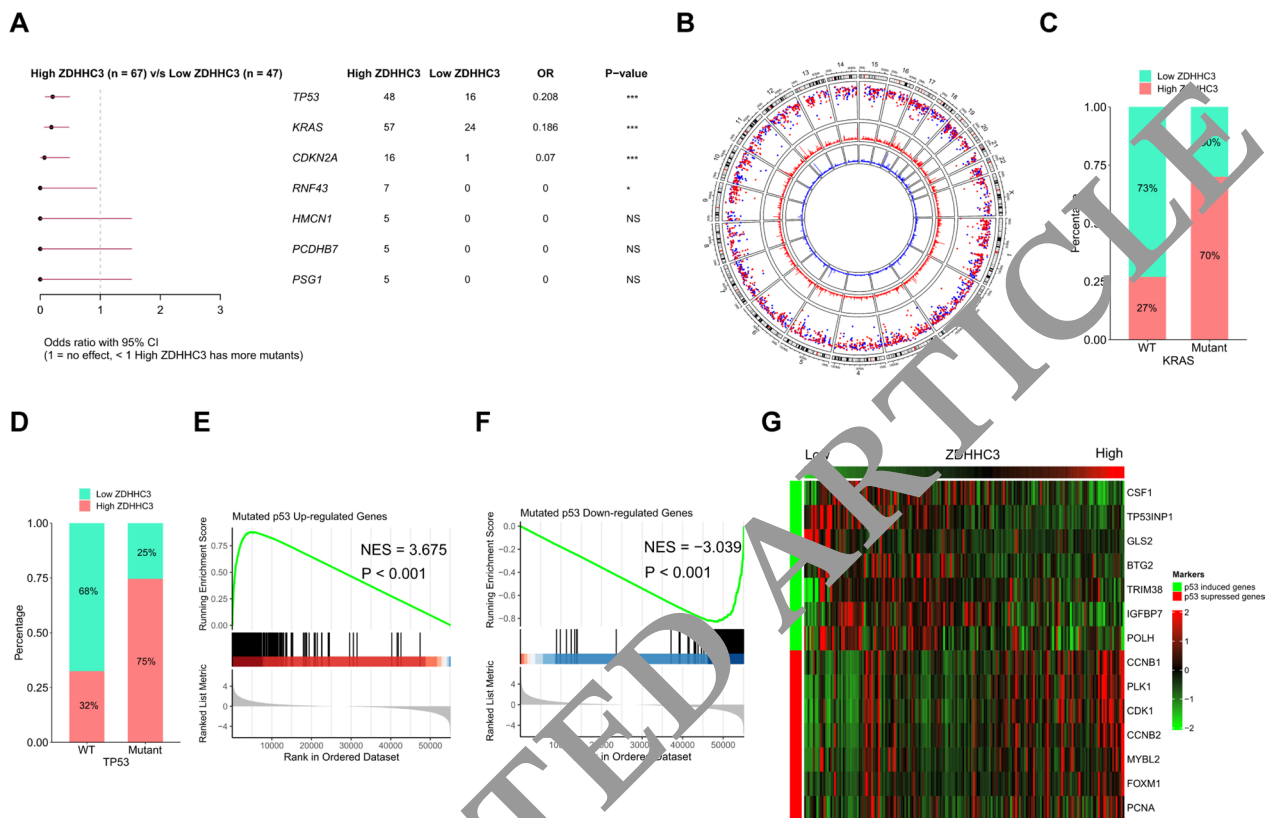
Fig. 5 Comparison of mutation landscape between PAAD patients with high and low ZDHHC3 expression. **A** Forest plot showing the most significant mutant genes in ZDHHC3-high and ZDHHC3-low PAAD tumors. **B** Circular plot showing the mutation status of ZDHHC3-high and ZDHHC3-low PAAD tumors. The genomic density of mutation genes in ZDHHC3-high tumors, in ZDHHC3-low tumors. **C**, **D** Proportion of PAAD patients harboring wildtype or mutant KRAS (**C**) or TP53 (**D**). **E**, **F** GSEA of genes up- (**E**) or downregulated (**F**) in association with mutated KRAS, based on ZDHHC3 expression. **G** Heat map showing the correlation of ZDHHC3 gene expression and the expression of p53-induced genes or p53-suppressed genes in PAAD tumors. The heat map color indicates the correlation coefficient. Red color, positive correlations; green color, negative correlations (*ns*, not significant, *$p < 0.05$, and ***$p < 0.001$)

(See figure on next page.)

Fig. 6 Knockdown of ZDHHC3 expression suppresses tumor growth and induces immune effector cell infiltration in Panc 02 tumors. **A** Western blot assay detecting the protein level of ZDHHC3 in Panc 02 cells that were transfected with the control-shRNA or ZDHHC3-shRNA; the stable clones were used in subsequent experiments. **B** Subcutaneous tumor growth curves: 5×10^6 stably-expressing shZDHHC3 Panc 02 cells or shControl Panc 02 cells were injected in the right flank of C57BL6/J mice ($n = 8$ mice per group). **C**, **D** The tumor weight (**C**) and survival rate (**D**) of shControl and shZDHHC3 Panc 02 tumors were recorded at the end of the experiment. **E**–**H** The tumor tissues at the end point were digested into single-cell suspension and analyzed by flow cytometry. Then, cells were gated on single cells and selected on Live/Dead dye staining. Only live cells were included in the further analysis. Flow cytometry analysis of the number of NK cells (CD45^{+} CD3^{−}NK1.1^{+}) (**E**), CD8^{+} T cells (CD45^{+} CD8^{+}), CD4^{+} T cells (CD45^{+} CD4^{+}) (**F**), DCs (CD45^{+} CD11b^{+}CD11c^{+}) (**G**), type 1 macrophages (M1) (CD45^{+} CD11b^{+} F4/80^{+} CD206^{−}), and type 2 macrophages (M2) (CD45^{+} CD11b^{+} F4/80^{+} CD206^{+}) (**H**) infiltrating subcutaneous tumors, namely shControl and shZDHHC3 Panc 02 tumors at day 23. Percentages indicate different immune cell populations amongst live CD45^{+} immune cells. **I** Western blot assay detecting the protein level of PD-L1 in control, ZDHHC3-knockdown, and ZDHHC3-knockdown with PD-L1 overexpressed Panc 02 cells; the stable clones were used in subsequent experiments. **J** Subcutaneous tumor growth curves: 5×10^6 stably-expressing (Control, shZDHHC3, and shZDHHC3 + PD-L1) Panc 02 cells were injected in the right flank of C57BL6/J mice ($n = 6$ mice per group). **K**, **L** The tumor weight (**K**) and survival rate (**L**) of (Control, shZDHHC3, and shZDHHC3 + PD-L1) Panc 02 tumors were recorded at the end of the experiment. Survival curves from the subcutaneous Panc 02 tumor model were developed until the animal's death or the tumor volume reached > 1000 mm³. Mice were euthanized when the calculated tumor size reached ~ 1000 mm³ or when tumors became ulcerated. Survival curves were analyzed using the log-rank (Mantel-Cox) test. Results shown are presented as mean ± SEM. (*ns*, not significant, *$p < 0.05$, and **$p < 0.01$)
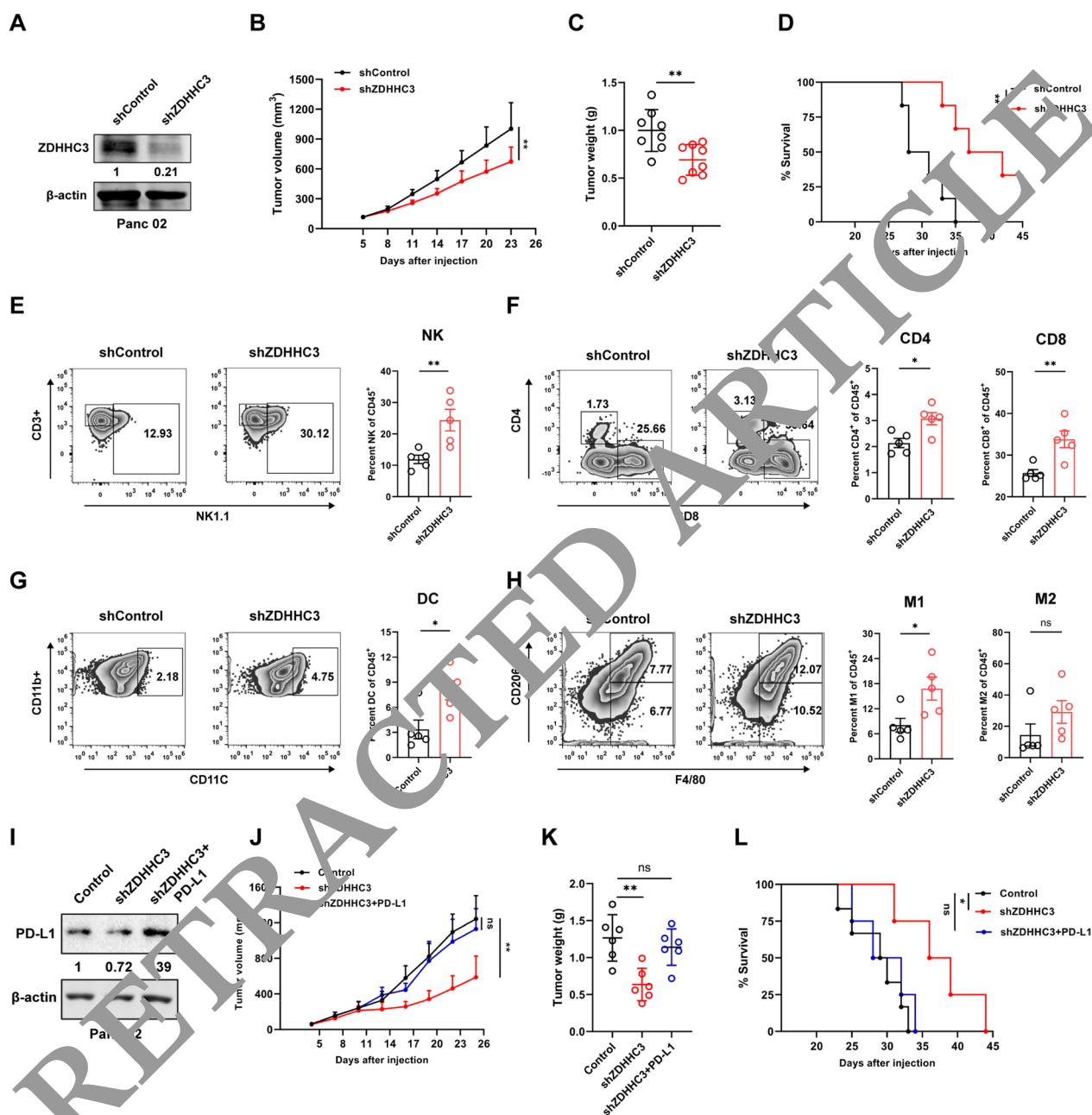
Fig. 6 (See legend on previous page.)

show that ZDHHC3 deficiency can inhibit pancreatic cancer progression by enhancing anti-tumor immunity.

2-BP impairs cell viability and sphere-forming activities, as well as increases apoptosis of pancreatic cancer cells

Next, we wanted to determine whether ZDHHCs can be targeted as a therapeutic tool for pancreatic cancer, Panc 02 and PANC-1 pancreatic cancer cell lines were treated with 2-bromopalmitate (2-BP), a ZDHHC-specific

inhibitor. We found that 2-BP treatment significantly induced apoptosis of Panc 02 cells in a dose-dependent manner using the Annexin V-FITC/PI staining assay, and significantly early apoptosis of PANC-1 cells could also be observed with the 2-BP treatment at 100 μM concentrations (Fig. 7A, B). Moreover, 2-BP treatment suppressed cell viability of Panc 02 and PANC-1 pancreatic cancer cells in a time-dependent manner (Fig. 7C, D). At the same time, 2-BP can also inhibit the migration of Panc 02 and PANC-1 cells (Fig. 7E, F). Pancreatic cancer cells

vary in their tumorigenic properties with the presence of a subset pancreatic cancer stem cells (CSCs), which are more resistant to currently used therapeutic agents [47]. We further examined whether 2-BP could inhibit pancreatic CSCs using the single-cell tumor sphere formation assay. Under free-floating tumor sphere culture conditions, 2-BP significantly reduced the sphere formation capacity of pancreatic CSCs in a dose-dependent manner (Fig. 7G, H). The expression level of stemness markers, ALDH1, Nanog, OCT4, and SOX2 was also downregulated by 100 μM 2-BP treatment in two pancreatic CSCs (Fig. 7I, J). Previous studies have determined that mTOR signaling plays a key role in maintaining stemness of pancreatic cancer stem cells and helps cancer cells to survive [48]. As shown in Fig. 7I, J, 2-BP treatment inhibited the self-renewal ability of pancreatic cancer stem cells by inhibiting phosphorylation of mTOR. To assess whether 2-BP treatment has any effect on normal pancreatic ductal epithelial cell. A human pancreatic ductal epithelial cell line (HPDE6-C7) was assayed for cell viability after exposure to 100 μM 2-BP. 2-BP treatment did not elicit significant apoptosis on HPDE6-C7 cells (Fig. 7K). Meanwhile, no significant effect of 2-BP treatment on HPDE6-C7 cell migration and proliferation, or cell cycle was observed (Fig. 7L–N). Taken together, these results suggest that 2-BP selectively exhibit high toxicity against pancreatic cancer cells but not against normal pancreatic ductal epithelial cell.

2-BP shows potent therapeutic effect in Panc 02 tumor model

To get potentially useful information for the development of pharmacological approaches against pancreatic tumor, we assessed the effects of the specific S-palmitoylation inhibitor, 2-BP, on Panc 02 syngeneic pancreatic tumor growth. The treatment was started when the tumor volume reached 100 mm^3, and 8 mice were sorted into each group. 2-BP (50 mg kg^{-1}; one injection per day) or vehicle was given intraperitoneally continuously for 12 days and tumor volume was monitored every 3 days (Fig. 8A). Notably, as shown in Fig. 8B–D, 2-BP treatment significantly impeded tumor progression and reduced tumor

burden in Panc 02-bearing mice. We observed that the effect of 2-BP injection decreased PD-L1 expression and increased the granzyme B (GZMB) expression, indicating enhanced anti-tumor immunity (Fig. 8E–G). Notably, in comparison to the control group, 2-BP treatment significantly augmented an infiltration of CD8$^+$ cells into Panc 02 tumors (Fig. 8F–I) as well as increased the expression of CCL5, CXCL9, and CXCL11, which are three important inflammatory cytokines accounting for the infiltration of CD8$^+$T cells and reshaping the inflammatory TME in pancreatic cancer (Fig. 8J) [49]. We also observed elevated secretion of CCL5 and CXCL9, but not CCL4 and CXCL10 in 2-BP treated Panc 02 cells in vitro (Additional file 1: Fig. S13). Together, our results suggest the use of a specific ZDHHCs inhibitor, 2-BP as a potential pharmacological tool for pancreatic cancer treatment.

2-BP enhances the therapeutic responsiveness of anti–PD-L1/PD-1 therapy in Panc 02 tumor model

We next investigated whether 2-BP could enhance the therapeutic efficacy of PD-1/PD-L1 checkpoint antibody blockade in pancreatic cancer. Therefore, we sought to determine the potential synergistic therapeutic effect of 2-BP and PD-1/L1 inhibitor in poorly immunogenic Panc 02 tumor model, characterized by a low proportion of tumor infiltrating lymphocytes with resistance to anti-PD-1/PD-L1 therapy [50]. An anti-PD-1/L1 antibody or isotype control (IgG2a) was injected (200 μg, intraperitoneally) twice a week after the subcutaneous 5×10^6 Panc 02 cells injection, with 2-BP or vehicle intraperitoneally at a dose of 50 mg/kg daily for 12 consecutive days. Survival time was defined as the day of death or an estimated tumor size > 1000 mm^3. Strikingly, while the use of anti-PD-1 or anti-PD-L1 alone had almost no effect on Panc 02 tumor growth and mice survival time, the combination treatment of 2-BP and anti-PD-1 or anti-PD-L1 antibody markedly slowed tumor growth and prolonged the mice survival time (Fig. 9A–F). Importantly, the median survival of untreated Panc 02 mice was approximately 27 days, whereas the median survival of mice in the 2-BP plus

(See figure on next page.)

Fig. 7 2-BP suppresses pancreatic-tumor cell viability and tumor sphere-forming activities, as well as increases apoptosis in vitro. **A**, **B** The effect of 2-BP on the apoptosis of Panc 02 (**A**) and PANC-1 (**B**) cells were detected by flow cytometry. **C**, **D** The Panc 02 (**C**) and PANC-1 (**D**) cells were pre-treated with 2-BP for 24 h, then the cell viability was analyzed using the CCK8 cell proliferation assay kit. **E**, **F** The effect of 2-BP treatment on the migration of Panc 02 (**E**) and PANC-1 (**F**) cells were examined by scratch test. **G**, **H** Representative images showing Panc 02 (**G**) and PANC-1 (**H**) 3D tumor culture model maintained in tumorsphere conditions for 7 days with indicated 2-BP treatment. **I**, **J** Differences in the expression of stem cell markers (ALDH1, Nanog, OCT4, SOX2) and mTOR signaling in Panc 02 (**I**) and PANC-1 (**J**) tumor spheres treated with 2-BP was analyzed by Western blotting assay. **K** The effect of 2-BP on the apoptosis of HPDE6-C7 cells was detected by flow cytometry. **L** The effect of 2-BP treatment on the migration of HPDE6-C7 cells was examined by scratch test. **M** The effect of 2-BP treatment on the HPDE6-C7 cell proliferation was examined by CCK8 cell proliferation assay kit. **N** Cell cycle of HPDE6-C7 cells with or without 2-BP treatment was analyzed by flow cytometry. The percent of G0/G1 phase, S phase, and G2/M phase were determined. Results shown are presented as mean ± SD. (*ns*, not significant, *$p < 0.05$, **$p < 0.01$, and ***$p < 0.001$)
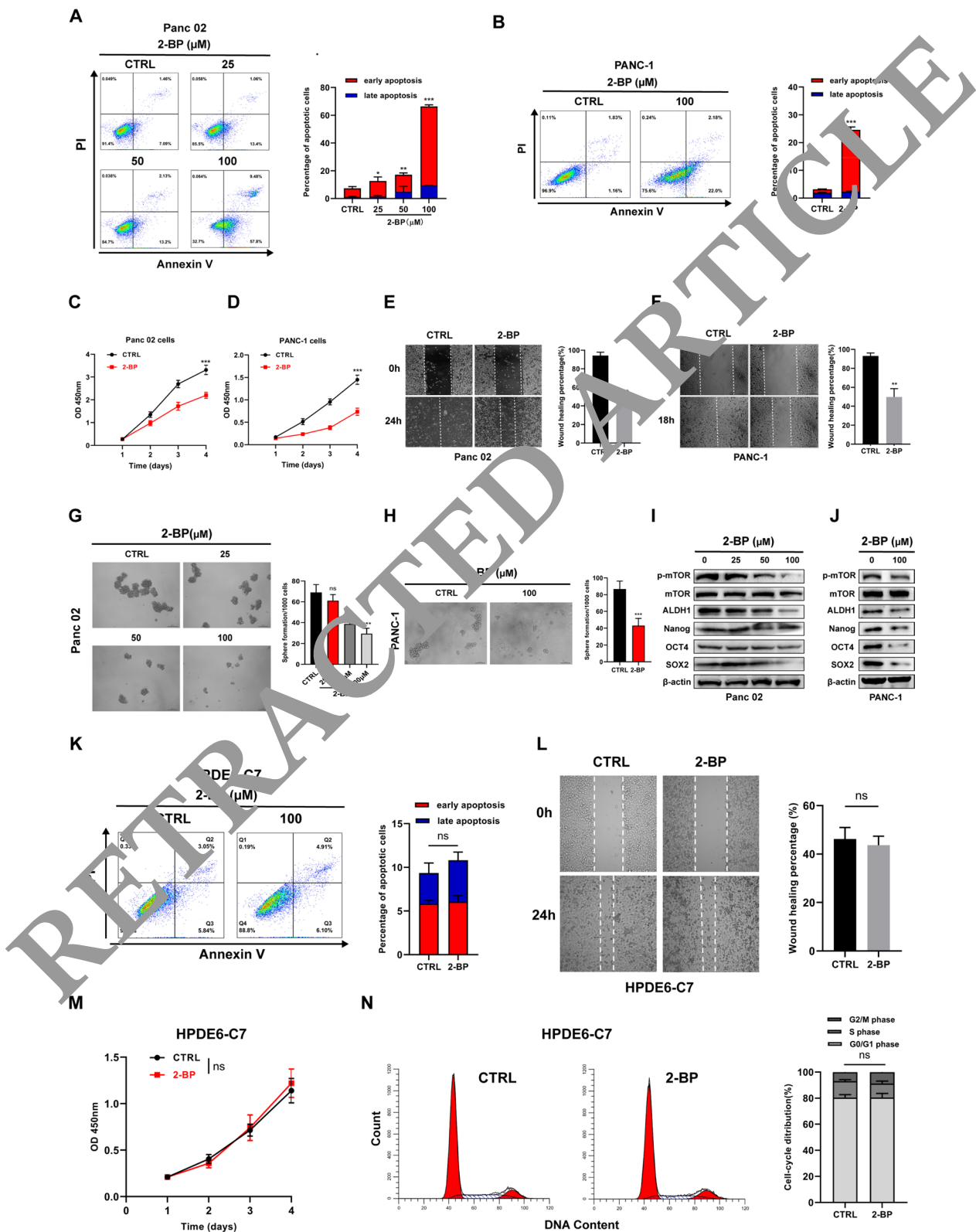
**Fig. 7** (See legend on previous page.)
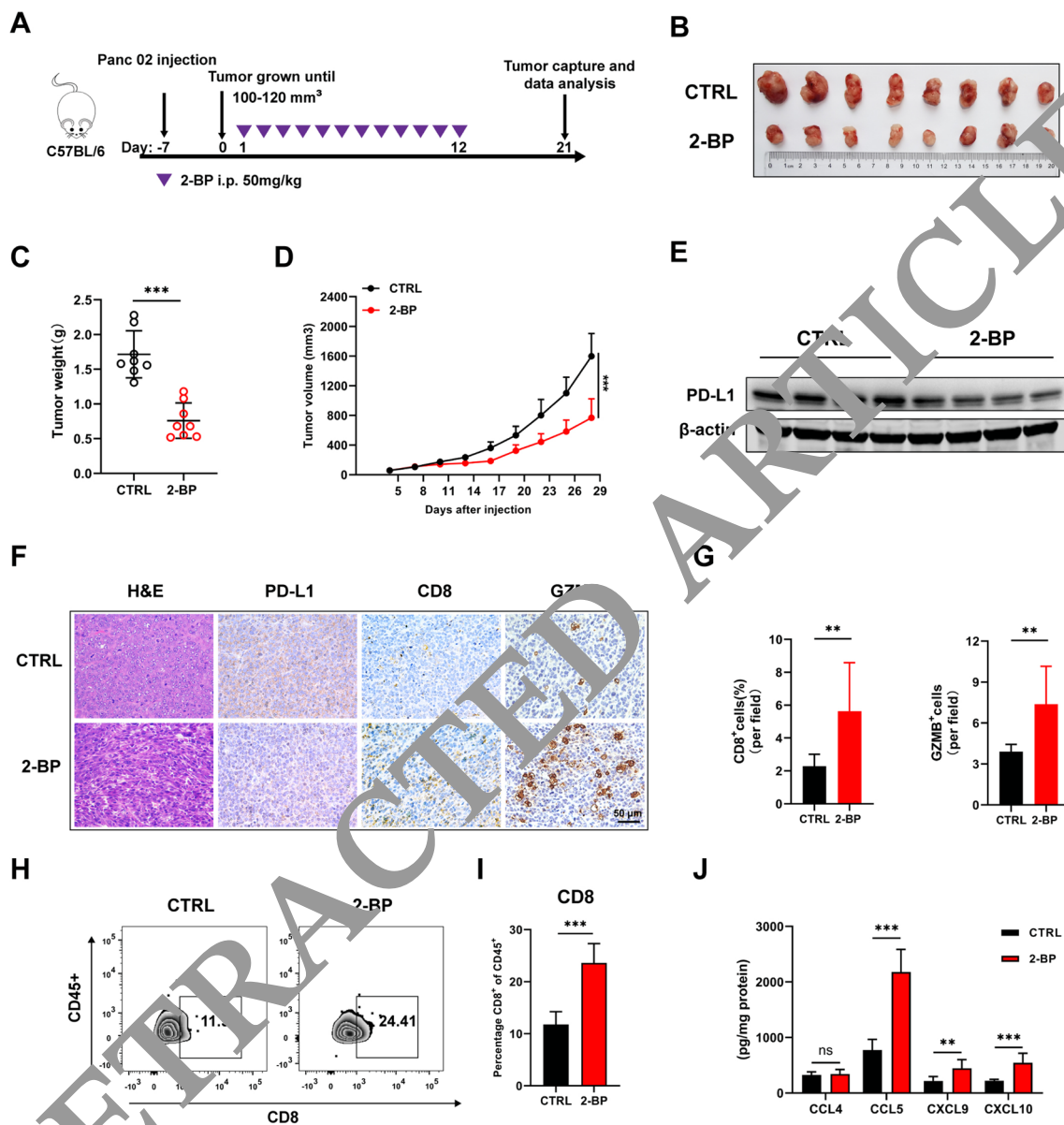
Fig. 8 2-BP delays tumor growth in Panc 02 tumor model. **A–D** Individual C57BL/6 mice were subcutaneously injected with 5×10^6 Panc 02 cells and received 2-BP treatment or Vehicle (CTRL). Schematic representation of treatment plan (**A**). Representative images of the tumors taken 28 days after injection, individuals' representative tumor of each group (**B**), tumor weight (**C**), and tumor growth curves (**D**) of Vehicle (CTRL) or 2-BP treated Panc 02 tumors ($n = 8$ mice per group). **E** Western blotting analysis showing the decreased PD-L1 protein expression in Panc 02 tumor tissues of mice treated with 2-BP (50 mg/kg) at the indicated time. **F, G** H&E and IHC staining (**F**) of PD-L1, CD8α, and GZMB in Panc 02 tumor tissues of mice treated by 2-BP (50 mg/kg) and quantification (**G**). **H, I** Flow cytometry analysis of the number of tumor-infiltrating CD8+ T cells (CD45+ CD8+) (**H**) in CTRL and 2-BP treated Panc 02 tumors and quantification (**I**). **J** Concentrations of CCL4, CCL5, CXCL9, and CXCL10 in CTRL and 2-BP treated Panc 02 tumor tissues were measured by ELISA. Results shown are presented as mean ± SD. (*ns*, not significant, **p < 0.01, and ***p < 0.001)

anti-PD-1 and 2-BP plus anti-PD-L1 co-treatment groups was 78 and 49 days, respectively (Fig. 9C, F). The combination therapy was well-tolerated and no significant weight loss was observed during the treatment period. Taken together, our results indicated that inhibition of palmitoyl transferases by 2-BP can render nonresponsive Panc 02 tumor-bearing mice responsive to anti-PD-1/PD-L1 therapy.

Discussion

The palmitoylation status of specific tumor-related proteins can be regulated by selectively manipulating ZDHHCs to finely promote tumorigenesis or tumor suppression. Therefore, ZDHHCs-mediated palmitoylation that is frequently altered in the tumor microenvironment represents promising targets for cancer therapy. Importantly, genetic inhibition of ZDHHCs (ZDHHC3,

Lin *et al. Journal of Translational Medicine*   (2023) 21:249

Page 20 of 24
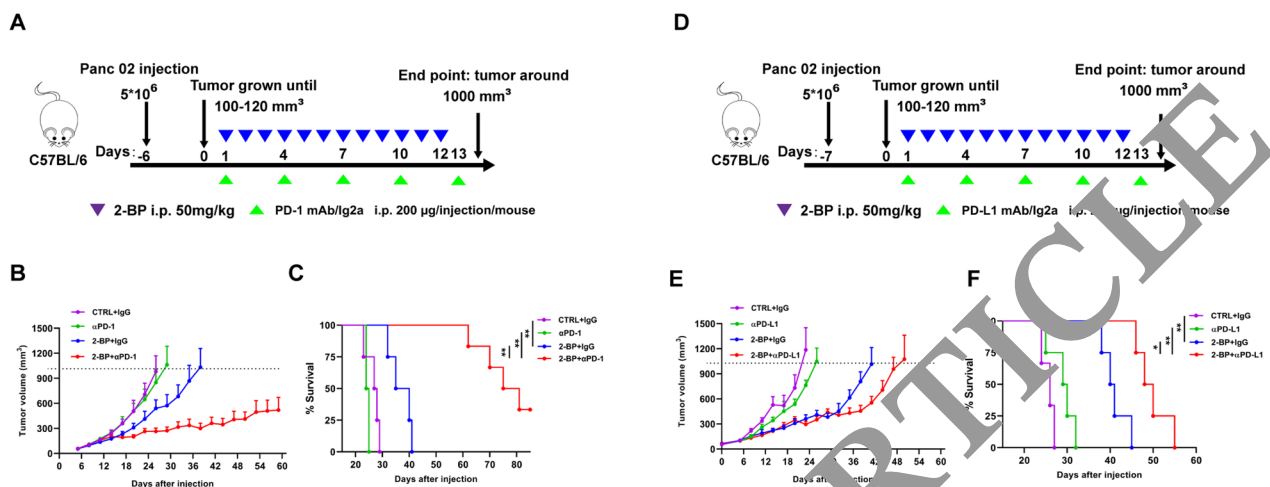
Fig. 9 Improved in vivo anti-tumor effect of 2-BP and PD-1/ PD-L1 blockade cotreatment. **A–C** Male C57BL/6 mice were injected subcutaneously with 5×10^6 Panc 02 cells, then, the tumor bearing mice were co-treated with 2-BP and anti-PD-1 antibody or IgG isotype control. Schematic representation of experimental plan (**A**). Tumor volume growth curves (**B**) and survival curves of the mice bearing Panc 02 tumors with the indicated treatment ($n = 6$ mice per group). **D–F** Male C57BL/6 mice were subcutaneously injected with 5×10^6 Panc 02 cells, then, the tumor bearing mice were co-treated with 2-BP and anti-PD-L1 antibody or isotype control IgG. Schematic representation of experimental plan (**D**). Tumor volume growth curves (**E**) and survival curves (**F**) of the mice bearing Panc 02 tumors with the indicated treatment ($n = 6$ mice per group). Survival curves with time were developed until the animal's death or the tumor volume reached > 1000 mm³. Differences between survival curves were analyzed using the log-rank (Mantel-Cox) test. Results shown are presented as mean ± SD. (*$p < 0.05$ and **$p < 0.01$)

5, 17, 9, 12) has revealed significant therapeutic efficacy in some animal tumor models, including colon cancer, glioblastoma, leukemia, and ovarian cancer. However, the expression profile and function of these individual family members in pancreatic cancer remain undefined. In this work, we first screened the mRNA levels of ZDHHCs according to the TCGA-PAAD dataset. We found that six (ZDHHC3, ZDHHC4, ZDHHC5, ZDHHC7, ZDHHC9, and ZDHHC20) out of 23 ZDHHC family members were highly elevated at both transcriptional and protein levels in pancreatic cancer. Additionally, among these differently expressed ZDHHCs, ZDHHC3/4/7/9/20 expression was closely associated with pancreatic cancer patients' individual stages. Of note, High expression of ZDHHC3/5/9/18/20 and ZDHHC3/4/5/7/9/20 were associated with poor prognosis in overall survival and relapse-free survival, respectively. Taken together, we identified ZDHHC3/9 as two members of 23 ZDHHCs that were differentially expressed in pancreatic carcinoma and were closely associated with pathological stage and prognostic value. RNA sequencing data from 33 pan-cancerous tissues in the GEPIA database showed that the transcriptional level of ZDHHC3 was selectively elevated in pancreatic cancer, so we further analyzed and validated the potential function of ZDHHC3 in PAAD. The CPTAC dataset and HPA database also validated the significant increase in ZDHHC3 protein levels in human pancreatic cancer tissues. Previous studies have identified ZDHHC3 as a therapeutic target for colon cancer

and breast cancer [23, 24]. Mechanistically, ZDHHC3 could enhance tumor progression by increasing the level of palmitoylated modifications of PD-L1 in MC38 tumor models and support breast tumor progression by regulating cellular oxidative stress and senescence. These results and our findings reveal that ZDHHC3 might act as a prognostic biomarker and exert a tumor-promoting property in pancreatic cancer.

After exploring the expression patterns and prognostic values of ZDHHC3, we systematically analyzed its potential roles in the tumor immune microenvironment. In the TCGA-PAAD cohort, analysis of the immunological status revealed that ZDHHC3 expression levels were negatively correlated with the majority of immunostimulatory factors, MHC molecules, chemokines, and their ligands, indicating that ZDHHC3 may play a role in the highly immunosuppressive TME of pancreatic cancer. Cancer-immunity cycle can systematically analyze the multistep processes of the anti-tumor immune response and help to find potential molecular targets to enhance cancer immunotherapy [51]. Here, we noted that the ZDHHC3 gene expression is negatively correlated with several key processes of the tumor immune cycle and some immune cells infiltration including DC cells, NK cells, CD4$^+$ T cells, CD8$^+$ T cells, and macrophages. Meanwhile, ZDHHC3 expression was incompatible with PD-1, CTLA4, and LAG3 expression levels in some tumors, including pancreatic cancer, and suggested that the immunomodulatory effects of ZDHHC3

Lin *et al. Journal of Translational Medicine*   (2023) 21:249

Page 21 of 24

have the potential to be used in combination with these immune checkpoint blockade. Most patients with pancreatic cancer carry mutations in KRAS and TP53, and the production of these mutations creates a highly immunosuppressive tumor microenvironment specific to pancreatic cancer, including a large infiltration of the regulatory T cells (Treg) and myeloid derived suppressor cells (MDSCs), so current immune checkpoint blockade therapies have very limited efficacy [52, 53]. Our analysis of the mutational status of pancreatic cancer and ZDHHC3 expression revealed that pancreatic cancer patients with high expression of ZDHHC3 had a higher proportion of KRAS and TP53 mutations, and pancreatic cancer patients carrying KRAS and TP53 mutations also had significantly higher levels of ZDHHC3 expression. TP53 mutations in PAAD are associated with increased amplification of oncogenes, enhanced chromosomal instability, and a poor prognosis [54]. Given that ZDHHC3 potentially positively regulates the activities of mutant TP53, thus inhibiting ZDHHC3 may sensitize pancreatic tumors to anti-tumor treatments, including immunotherapy. The association and underlying molecular mechanism between TP53 mutations and high ZDHHC3 activity in pancreatic cancer need to be further investigated.

Further, we validated in a Panc 02 pancreatic cancer model that the knockdown of ZDHHC3 in tumor cells could delay tumor growth, which was associated with enhanced anti-tumor immune response. In line with the previous observation that the knockdown of ZDHHC3 enhanced CD8$^+$ T cell infiltration in MC38 tumors [23], we also observed a similar phenomenon in the Panc 02 tumor model. In addition, we observed significantly increased levels of infiltration of DC cells, NK cells, CD4$^+$ T cells, and M1 macrophages in ZDHHC3-knockdown tumors by flow cytometry analysis, further suggesting the activation of systemic anti-tumor immunity. These immune profiles in Panc 02 tumors are also consistent with our bioinformatics results of human PAAD samples based on ZDHHC3 expression. Interestingly, PD-L1 overexpression almost completely abolished the anti-tumor effects of ZDHHC3-knockdown on Panc 02 tumors, evidenced by increased tumor weight and decreased mice survival time. Our results also indicated that ZDHHC3 directly regulates PD-L1 expression at the protein level in pancreatic cancer cells. More importantly, overexpression of PD-L1 can almost abrogate the anti-cancer effect of ZDHHC3 knockdown on Panc 02 pancreatic tumor model, thus targeting ZDHHC3 may be a potential therapeutic approach to enhance anti-tumor immunotherapy. Future studies should focus on ZDHHC3 knockdown in combination with PD-1 or PD-L1 inhibitors in pancreatic cancer treatment strategies. Meanwhile, the major immune cell types involved in ZDHHC3-mediated tumor control need to be further identified.

Finally, we explored whether a pharmacological approach targeting palmitoyl transferases could be a potential therapeutic option for pancreatic cancer. We found that the palmitoyl transferase inhibitor, 2-BP, suppressed Panc 02/PANC-1 cell viability and tumor sphere-forming activities, as well as increased apoptosis in vitro with minimal effect on human pancreatic ductal epithelial cell line (HPDE6-C7). Meanwhile, intraperitoneal injection of 2-BP significantly delayed the growth of Panc 02 tumors and increased the anti-tumor immune response. More importantly, 2-BP can significantly improve the immune checkpoint blockade efficacy of anti-PD-1 or anti-PD-L1. In the absence of observed tumor suppression by PD-1 or anti-PD-L1 against pancreatic cancer in Panc 02 tumor model, synergistic treatment with 2-BP rendered tumors significantly sensitive to immune checkpoint blockade (ICB). Our results demonstrated that the palmitoyl transferase inhibitor, 2-BP, may be a novel and effective pharmacological tool against pancreatic cancer.

However, there are still some limitations in our present study. First, our analysis was based primarily on the transcriptional data of ZDHHCs, the prognostic value of these ZDHHC enzymes and its potential role in TME needs to be further determined in large human pancreatic cancer samples. Second, the Panc 02 subcutaneously transplanted tumor model does not fully mimic changes in tumor progression in human pancreatic cancer, and we plan to further validate the therapeutic value of targeting ZDHHC3 as well as 2-BP treatment in a spontaneous pancreatic cancer tumor model in the future study. Despite these limitations, our results provide insight into the potential function of ZDHHC family members in pancreatic carcinogenesis and progression and pharmacologically validated whether targeting ZDHHCs would significantly increase the efficacy of ICB in pancreatic cancer.

Conclusion

Overall, our results indicated that some of ZDHHC enzyme genes are related to the prognosis of pancreatic cancer, and demonstrated that ZDHHC3 plays a critical oncogenic role in pancreatic cancer progression. Moreover, combined 2-BP and PD-1/PD-L1 inhibition overcomed intrinsic resistance to immune checkpoint blockade in a mouse model of pancreatic cancer.

Abbreviations
PAAD   Pancreatic adenocarcinoma
TCGA   The Cancer Genome Atlas

Lin *et al. Journal of Translational Medicine*　　(2023) 21:249

Page 22 of 24

TPM	Transcript per million
HPA	Human Protein Atlas
OS	Overall survival
RFS	Relapse-free survival
GEO	Gene Expression Omnibus
IHC	Immunohistochemical
TIICs	Tumor-infiltrating immune cells
ICB	Immune checkpoint blockade
2-BP	2-bromopalmitate
PD-1	Programmed cell death 1
PD-L1	Programmed cell death ligand 1
ssGSEA	Single sample Gene Set Enrichment Analysis
CPTAC	Clinical Proteomic Tumor Analysis Consortium
CTLA-4	Cytotoxic T lymphocyte antigen 4
LAG-3	Lymphocyte activation gene 3
GSVA	Gene Set Variation Analysis
NK	Natural killer
ELISA	Enzyme-linked immunosorbent assay
co-IP	Co-immunoprecipitation
RT-qRCR	Real-time quantitative PCR
IF	Immunofluorescence
TMB	Tumor mutational burden
MSI	Microsatellite instability

Supplementary Information

The online version contains supplementary material available at https://doi.org/10.1186/s12967-023-04098-3.

Additional file 1: Fig. S1. Representative immunohistochemical images of ZDHHC family members in human pancreatic cancer tissue from the HPA database. **Fig. S2.** Relationship between expression levels of ZDHHC3/4/7/9/15/17/20/22 and pathological stages of PAAD patients. **A-H** The association between mRNA expression of ZDHHC and patients' individual cancer stages of PAAD from the GEPIA database. $p < 0.05$ is considered statistically significant. **Fig. S3.** Relationship between ZDH-HCs gene expression and pathological stages of PAAD patients. **A-O** The association between mRNA expression of ZDHHCs and patients' individual cancer stages of PAAD from the GEPIA database. **Fig. S4.** Univariate and multivariate cox regression were used to test prognostic significance of ZDHHCs in TCGA-PAAD datasets. **A-B** The effect of ZDHHCs expression on overall survival (OS) (**A**) and relapse-free survival (RFS) (**B**) from the K-M plotter database. **Fig. S5.** Association between ZDHHC3 expression and overall survival time in pan-cancer based on TCGA database. **Fig. S6.** Associations between ZDHHC3 expression and disease-specific survival in pan-cancers based on TCGA database. **Fig. S7.** Correlation between TMB or MSI and ZDHHC3 expression in pan-cancers. **A** A stick chart showing the correlation between the ZDHHC3 and TMB in different tumor types. The red curve represents the Spearman correlation coefficient, and the black value represents the range. **B** A stick chart showing the correlation between the ZDHHC3 and MSI in different tumor types. **Fig. S8.** Differentially expressed chemokines and paired receptors between high- and low-ZDHHC3 PAAD patients. **A** Boxplot showing the chemokines and paired receptors with significant expression differences between high- and low-ZDHHC3 groups in TCGA-PAAD cohort. **B** Boxplot showing the chemokines and paired receptors with no significant expression differences between high- and low-ZDHHC3 groups in TCGA-PAAD cohort. The R software ggpubr package was used to draw boxplots and perform Student's t-test statistical analyses. Results shown are presented as mean ± SD. (*ns*, not significant, *p < 0.05, **p < 0.01, and ***p < 0.001). **Fig. S9.** Mutation landscape between high- and low-ZDHHC3 in PAAD. A mutation landscape shows the differences in gene mutation frequencies in each set of PAAD samples using chi-square tests to classify the top 15 genes with the highest mutation frequencies according to the expression of ZDHHC3. **Fig. S10.** KEGG enrichment and pathway correlation analysis for ZDHHC3 in PAAD. **A** Top 20 KEGG enrichment pathways in PAAD. **B** The abscissa represents the distribution of the ZDHHC3 expression, and the ordinate represents the distribution of the pathway score. The density curve on the right represents the trend in distribution of the pathway immune score, the upper density curve represents the trend in distribution of the

ZDHHC3 expression. The value on the top represents the correlation *p* value, correlation coefficient and correlation calculation method. **Fig. S11.** Concentrations of CCL4, CCL5, CXCL9, and CXCL10 in shControl and shZD-HHC3 Panc 02 tumor tissues on day 23 after tumor inoculation measured by ELISA. Results shown are presented as mean ± SD. (*ns*, not significant, *p < 0.05, and **p < 0.01). **Fig. S12**. ZDHHC3 knockdown inhibit PD-L1 expression at protein level in pancreatic cancer cells. (A-D) PANC-1 cell were transfected with siRNA. After 72 h, cells were harvested for (A) western blotting analysis, (B) RT-qPCR analysis, (C) flow cytometry assay and (D) corresponding quantification. (E) Representative immunofluorescence images of ZDHHC3 (green) and PD-L1 (red) staining of PANC-1 cells (blue, DAPI-labelled cell nuclei) and (F) corresponding quantification (Scale bars, 20 μm). (G) Reciprocal co-IP assay was performed to examine the interaction between endogenously expressed ZDHHC3 and PD-L1 in PANC-1 cells. Results shown are presented as mean ± SD. (*ns*, not significant and ***p < 0.001). **Fig. S13.** Relative expression of CCL4, CCL5, CXCL9, and CXCL10 in CTRL and 2-BP treated Panc 02 cells *in vitro*. Concentrations of CCL4, CCL5, CXCL9, and CXCL10 in CTRL and 2-BP treated Panc 02 cells for 24 h were measured by ELISA. Results shown are presented as mean ± SD. (*ns*, not significant and ***p < 0.001).

Availability of data and materials
The datasets generated during and/or analyzed during the current study are available on reasonable request.

Declarations

Ethics approval and consent to participate
This study was reviewed and approved by the school of Ophthalmology & Optometry, Eye Hospital, Wenzhou Medical University Ethics Committee. All animal experimental procedures were approved by Laboratory Animal Ethics Committee of Wenzhou Medical University.

Consent for publication
All authors have read and approved the content and agree to submit for consideration for publication in the journal.

Competing interests
The authors declare that they have no known competing financial interests.

References

1. Schizas D, Charalampakis N, Kole C, Economopoulou P, Koustas E, Gkotsis E, Ziogas D, Psyrri A, Karamouzis MV. Immunotherapy for pancreatic cancer: a 2020 update. Cancer Treat Rev. 2020;86: 102016.
2. Bliss LA, Witkowski ER, Yang CJ, Tseng JF. Outcomes in operative management of pancreatic cancer. J Surg Oncol. 2014;110:592–8.
3. Ilic M, Ilic I. Epidemiology of pancreatic cancer. World J Gastroenterol. 2016;22:9694–705.
4. Sahin IH, Askan G, Hu ZI, O'Reilly EM. Immunotherapy in pancreatic ductal adenocarcinoma: an emerging entity? Ann Oncol. 2017;28:2950–61.

Lin *et al. Journal of Translational Medicine*   (2023) 21:249

Page 23 of 24

5.   Pietrobon V, Marincola FM. Hypoxia and the phenomenon of immune exclusion. J Transl Med. 2021;19:9.

6.   Neesse A, Bauer CA, Öhlund D, Lauth M, Buchholz M, Michl P, Tuveson DA, Gress TM. Stromal biology and therapy in pancreatic cancer: ready for clinical translation? Gut. 2019;68:159–71.

7.   Ullman NA, Burchard PR, Dunne RF, Linehan DC. Immunologic strategies in pancreatic cancer: making cold tumors hot. J Clin Oncol. 2022;40:2789–805.

8.   Maggs L, Ferrone S. Improving the clinical significance of preclinical immunotherapy studies through incorporating tumor microenviron-ment-like conditions. Clin Cancer Res. 2020;26:4448–53.

9.   Dong H, Strome SE, Salomao DR, Tamura H, Hirano F, Flies DB, Roche PC, Lu J, Zhu G, Tamada K, et al. Tumor-associated B7–H1 promotes T-cell apoptosis: a potential mechanism of immune evasion. Nat Med. 2002;8:793–800.

10. Chen L, Han X. Anti-PD-1/PD-L1 therapy of human cancer: past, present, and future. J Clin Invest. 2015;125:3384–91.

11. O'Reilly EM, Oh DY, Dhani N, Renouf DJ, Lee MA, Sun W, Fisher G, Hezel A, Chang SC, Vlahovic G, et al. Durvalumab with or without tremelimumab for patients with metastatic pancreatic ductal adenocarcinoma: a phase 2 randomized clinical trial. JAMA Oncol. 2019;5:1431–8.

12. Zhang Y, Qin Z, Sun W, Chu F, Zhou F. Function of protein S-palmitoylation in immunity and immune-related diseases. Front Immunol. 2021;12: 661202.

13. Blanc M, David F, Abrami L, Migliozzi D, Armand F, Burgi J, van der Goot FG. SwissPalm: protein palmitoylation database. F10000 Res. 2015;4:261.

14. Fukata Y, Murakami T, Yokoi N, Fukata M. Local palmitoylation cycles and specialized membrane domain organization. Curr Top Membr. 2016;77:97–141.

15. Greaves J, Chamberlain LH. DHHC palmitoyl transferases: substrate inter-actions and (patho)physiology. Trends Biochem Sci. 2011;36:245–53.

16. Lanyon-Hogg T, Faronato M, Serwa RA, Tate EW. Dynamic protein acyla-tion: new substrates, mechanisms, and drug targets. Trends Biochem Sci. 2017;42:566–81.

17. Sanders SS, Martin DD, Butland SL, Lavallee-Adam M, Calzolari D, Kay C, Yates JR 3rd, Hayden MR. Curation of the mammalian palmitoylome indicates a pivotal role for palmitoylation in diseases and disorders of the nervous system and cancers. PLoS Comput Biol. 2015;11:e1004405.

18. Jin J, Zhi X, Wang X, Meng D. Protein palmitoylation and its pathophysi-ological relevance. J Cell Physiol. 2021;236:3220–33.

19. Lin H. Protein cysteine palmitoylation in immunity and inflammation. FEBS J. 2021;288:7043–59.

20. Greaves J, Chamberlain LH. New links between S-acylation and cancer. J Pathol. 2014;233:4–6.

21. Ko PJ, Dixon SJ: **Protein palmitoylation and cancer.** *EMBO Rep* 2018, **19**.

22. Yeste-Velasco M, Linder ME, Lu YJ. Protein S-palmitoylation and cancer. Biochim Biophys Acta. 2015;1856:107–20.

23. Yao H, Lan J, Li C, Shi H, Brosseau JP, Wang H, Lu H, Fang C, Zhang Y, Liang L, et al. Inhibiting PD-L1 palmitoylation enhances T-cell immune responses against tumours. Nat Biomed Eng. 2019;3:306–17.

24. Sharma C, Wang HX, Li Q, Knoblich K, Reisenbichler ES, Richardson AL, Hemler ME. Protein acyltransferase DHHC3 regulates breast tumor growth, oxidative stress, and senescence. Cancer Res. 2017;77:6880–90.

25. Tian H, Lu JY, Shao C, Huffman KE, Carstens RM, Larsen JE, Girard L, Liu H, Rodriguez-Canales J, Frenkel EP, et al. Systematic siRNA screen unmasks NSCLC growth dependence by palmitoyltransferase DHHC5. Mol Cancer Res. 2015;13:784–94.

26. Chen X, Ma H, Wang Z, Zhang S, Yang H, Fang Z. EZH2 palmitoylation mediated by ZDHHC5 in p53-mutant glioma drives malignant develop-ment and progression. Cancer Res. 2017;77:4998–5010.

27. Chen X, Hao A, Li X, Ye K, Zhao C, Yang H, Ma H, Hu L, Zhao Z, Hu L, et al. Activation of JNK and p38 MAPK mediated by ZDHHC17 drives glioblas-toma multiforme development and malignant progression. Theranostics. 2020;10:998–1015.

28. Liu P, Jiao B, Zhang R, Zhao H, Zhang C, Wu M, Li D, Zhao X, Qiu Q, Li J, Ren R. Palmitoylacyltransferase Zdhhc9 inactivation mitigates leukemo-genic potential of oncogenic Nras. Leukemia. 2016;30:1225–8.

29. Zhang Z, Li X, Yang F, Chen C, Liu P, Ren Y, Sun P, Wang Z, You Y, Zeng YX, Li X. DHHC9-mediated GLUT1 S-palmitoylation promotes glioblastoma glycolysis and tumorigenesis. Nat Commun. 2021;12:5872.

30. Yuan M, Chen X, Sun Y, Jiang L, Xia Z, Ye K, Jiang H, Yang B, Ying M, Cao J, He Q. ZDHHC12-mediated claudin-3 S-palmitoylation determines ovarian cancer progression. Acta Pharm Sin B. 2020;10:1426–39.

31. Chen S, Zhu B, Yin C, Liu W, Han C, Chen B, Liu T, Li X, Chen X, Li C, et al. Palmitoylation-dependent activation of MC1R prevents melanomagen-esis. Nature. 2017;549:399–403.

32. Tang Z, Li C, Kang B, Gao G, Li C, Zhang Z. GEPIA: a web server for cancer and normal gene expression profiling and interactive analyses. Nucleic Acids Res. 2017;45:W98–102.

33. Barrett T, Wilhite SE, Ledoux P, Evangelista C, Kim IF, Tomashevsky M, Marshall KA, Phillippy KH, Sherman PM, Holko M, et al. NCBI GEO: archive for functional genomics data sets—update. Nucleic Acids Res. 2013;41:D991-995.

34. Chandrashekar DS, Bashel B, Balasubramanya SAH, Creighton CJ, Ponce-Rodriguez I, Chakravarthi B, Varambally S. UALCAN: a portal for facilitating tumor subgroup gene expression and survival analyses. Neoplasia. 2017;19:649–58.

35. Nagy A, Munkacsy G, Gyorffy B. Pancancer survival analysis of cancer hallmark genes. Sci Rep. 2021;11:6047.

36. Huang K, Lin Z, Ge Y, Chen X, Pan Y, Lv Z, Sun X, Yu H, Chen J, Yao Q. Immunomodulation of MiRNA-223-based nanoplatform for targeted therapy in retinopathy of prematurity. J Control Release. 2022;350:789–802.

37. Huang K, Li X, Lv Z, Zhang D, Zhou Y, Lin Z, Guo J. MMP9-responsive graphene oxide quantum dot-based nano-in-micro drug delivery system for combinatorial therapy of choroidal neovascularization. Small. 2023;2023:e2207335.

38. Wellenstein MD, de Visser KE. Cancer-cell-intrinsic mechanisms shaping the tumor immune landscape. Immunity. 2018;48:399–416.

39. Ayers M, Lunceford J, Nebozhyn M, Murphy E, Loboda A, Kaufman DR, Albright A, Cheng JD, Kang SP, Shankaran V, et al. IFN-gamma-related mRNA profile predicts clinical response to PD-1 blockade. J Clin Invest. 2017;127:2930–40.

40. Charoentong P, Finotello F, Angelova M, Mayer C, Efremova M, Rieder D, Hackl H, Trajanoski Z. Pan-cancer immunogenomic analyses reveal genotype-immunophenotype relationships and predictors of response to checkpoint blockade. Cell Rep. 2017;18:248–62.

41. Chen DS, Mellman I. Oncology meets immunology: the cancer-immunity cycle. Immunity. 2013;39:1–10.

42. Hu J, Yu A, Othmane B, Qiu D, Li H, Li C, Liu P, Ren W, Chen M, Gong G, et al. Siglec15 shapes a non-inflamed tumor microenvironment and predicts the molecular subtype in bladder cancer. Theranostics. 2021;11:3089–108.

43. Gupta R, Amanam I, Chung V. Current and future therapies for advanced pancreatic cancer. J Surg Oncol. 2017;116:25–34.

44. Lenkiewicz E, Malasi S, Hogenson TL, Flores LF, Barham W, Phillips WJ, Roesler AS, Chambers KR, Rajbhandari N, Hayashi A, et al. Genomic and epigenomic landscaping defines new therapeutic targets for adenosqua-mous carcinoma of the pancreas. Cancer Res. 2020;80:4324–34.

45. Spranger S, Dai D, Horton B, Gajewski TF. Tumor-residing Batf3 dendritic cells are required for effector T Cell trafficking and adoptive T cell therapy. Cancer Cell. 2017;31:711-723.e714.

46. Tang W, Xu N, Zhou J, He Z, Lenahan C, Wang C, Ji H, Liu B, Zou Y, Zeng H, Guo H. ALKBH5 promotes PD-L1-mediated immune escape through m6A modification of ZDHHC3 in glioma. Cell Death Discov. 2022;8:497.

47. Valle S, Alcala S, Martin-Hijano L, Cabezas-Sainz P, Navarro D, Munoz ER, Yuste L, Tiwary K, Walter K, Ruiz-Canas L, et al. Exploiting oxidative phosphorylation to promote the stem and immunoevasive properties of pancreatic cancer stem cells. Nat Commun. 2020;11:5265.

48. Miyazaki Y, Matsubara S, Ding Q, Tsukasa K, Yoshimitsu M, Kosai K, Takao S. Efficient elimination of pancreatic cancer stem cells by hedgehog/GLI inhibitor GANT61 in combination with mTOR inhibition. Mol Cancer. 2016;15:49.

49. Romero JM, Grunwald B, Jang GH, Bavi PP, Jhaveri A, Masoomian M, Fischer SE, Zhang A, Denroche RE, Lungu IM, et al. A four-chemokine signature is associated with a T-cell-inflamed phenotype in primary and metastatic pancreatic cancer. Clin Cancer Res. 2020;26:1997–2010.

50. Lv H, Lv G, Chen C, Zong Q, Jiang G, Ye D, Cui X, He Y, Xiang W, Han Q, et al. NAD(+) metabolism maintains inducible PD-L1 expression to drive tumor immune evasion. Cell Metab. 2021;33(110–127): e115.

51. Chen DS, Mellman I. Elements of cancer immunity and the cancer-immune set point. Nature. 2017;541:321–30.
52. Hashimoto S, Furukawa S, Hashimoto A, Tsutaho A, Fukao A, Sakamura Y, Parajuli G, Onodera Y, Otsuka Y, Handa H, et al. ARF6 and AMAP1 are major targets of KRAS and TP53 mutations to promote invasion, PD-L1 dynamics, and immune evasion of pancreatic cancer. Proc Natl Acad Sci USA. 2019;116:17450–9.
53. Zhang X, Mao T, Zhang B, Xu H, Cui J, Jiao F, Chen D, Wang Y, Hu J, Xia Q, et al. Characterization of the genomic landscape in large-scale Chinese patients with pancreatic cancer. EBioMedicine. 2022;77: 103897.
54. Donehower LA, Soussi T, Korkut A, Liu Y, Schultz A, Cardenas M, Li X, Babur O, Hsu TK, Lichtarge O, et al. Integrated analysis of TP53 gene and pathway alterations in the cancer genome atlas. Cell Rep. 2019;28(1370–1384): e1375.

Publisher's Note